Paleobiology, 49(1), 2023, pp. 77–98
DOI: 10.1017/pab.2022.24

PALEOBIOLOGY
A PUBLICATION OF THE Paleontological SOCIETY

Article

Small but mighty: how overlooked small species maintain community structure through middle Eocene climate change

*L. E. Kearns**, *S. M. Bohaty*, *K. M. Edgar*, *and T. H. G. Ezard*

Abstract.—Understanding current and future biodiversity responses to changing climate is pivotal as anthropogenic climate change continues. This understanding is complicated by the multitude of available metrics to quantify dynamics and by biased sampling protocols. Here, we investigate the impact of sampling protocol strategies using a data-rich fossil record to calculate effective diversity using Hill numbers for the first time on Paleogene planktonic foraminifera. We sample 22,830 individual tests, in two different size classes, across a 7 Myr time slice of the middle Eocene featuring a major transient warming event, the middle Eocene climatic optimum (MECO; ~40 Ma), at study sites in the midlatitude North Atlantic. Using generalized additive models, we investigate community responses to climatic fluctuations. After correcting for any effects of fossil fragmentation, we show a peak in generic diversity in the early and middle stages of the MECO as well as divergent trajectories between the typical size-selected community (>180 μm) and a broader assemblage, including smaller genera (>63 μm). Assemblages featuring smaller genera are more resilient to the climatic fluctuations of the MECO than those assemblages that feature only larger genera, maintaining their community structure at the reference Hill numbers for Shannon's and Simpson's indices. These results raise fundamental questions about how communities respond to climate excursions. In addition, our results emphasize the need to design studies with the aim of collecting the most inclusive data possible to allow detection of community changes and determine which species are likely to dominate future environments.

L. E. Kearns, S. M. Bohaty, and T. H. G. Ezard. School of Ocean and Earth Science, National Oceanography Centre Southampton, University of Southampton Waterfront Campus, Southampton SO14 3ZH, U.K.
E-mail: L.Kearns@soton.ac.uk, S.Bohaty@noc.soton.ac.uk, T.Ezard@soton.ac.uk

K. M. Edgar. School of Geography, Earth and Environmental Sciences, University of Birmingham, Birmingham B15 2TT, U.K. E-mail: k.m.edgar@bham.ac.uk

Accepted: 20 June 2022
*Corresponding author.

Introduction

Biodiversity is multifaceted; so how should it be summarized succinctly? The ubiquitous starting point is to generate records of taxic abundance resulting in records of richness. Species are regarded by many researchers as the most intuitive unit of biology and the fundamental measure of diversity (e.g., Colwell et al. 1994; Purvis and Hector 2000; Mace et al. 2012; Hohenegger 2014), making species the most common currency for diversity studies. This preference for species-level studies is a result of species being argued to have independent evolutionary trajectories and histories (Purvis and Hector 2000) understandable to both researchers and the general public (Purvis and Hector 2000; Baum 2009; Chiarucci et al. 2011; Reydon 2019), which can aid conservation and public engagement efforts. Despite this preference, species do not represent a "silver bullet": species show different amounts of intraspecific variation in the same ways as populations or genera. Genera also represent a biological reality (Mayr 1942) and share phenotypic and ecological traits (Aze et al. 2011). Furthermore, measuring diversity at the genus level means studies are less prone to identification error and more repeatable among different workers and the data is less prone to stochastic fluctuations that may or may not be of genuine biological interest (Hendricks et al. 2014). If the goal is a unit that

0094-8373/23

provides a robust summary of biodiversity change, genus-based levels provide an ecologically informative record of diversity in deep time (Hendricks et al. 2014).

Following taxonomic scale, the next choice is what to measure within the sample itself. Common taxa are abundant, by definition detectable, have a broad distribution (Hannisdal et al. 2017), and are also likely to be influential components of ecosystems (Lennon et al. 2004; Gaston 2008; Hannisdal et al. 2017). Thus, it is hypothesized that common taxa contribute more to assemblage diversity than rare taxa (Lennon et al. 2004; Gaston 2008). Furthermore, for a taxon to have become common, there must have been a complex interplay of traits and environmental influences, as well as historical and spatial dynamics (Gaston 2008), that are replicated for establishment to be sufficiently frequent. Common taxa should therefore be able to inform our understanding of the drivers of biodiversity dynamics.

Yet, to be common is in itself rare. Very few taxa across global biodiversity are common (Gaston and Fuller 2007; Gaston 2008; Hannisdal et al. 2017), so a large proportion of information is discarded when only common taxa are measured. Fluctuating abundances in rare taxa, that is, those with few individuals and geographically restricted distributions, may prove more ecologically informative, potentially acting as "ecosystem canaries" providing early warning signals for ecosystem collapse (Doncaster et al. 2016) and insights into paleoceanographic change (Ishino and Suto 2020) and acting as the focus of conservation efforts (Gaston 2008). However, taxa vary spatially, directly influencing ecological dynamics and diversity patterns within each generation at any single location only (Patzkowsky and Holland 2007). Consequently, what is rare in one sample or area may be common in another (Colwell 2009). Perhaps it is not what is rare that is important but instead what is absent from a sample, or so-called dark diversity (Pärtel et al. 2011). On a theoretical level, far less is known about the functional role of rare taxa in their ecosystems (Lyons et al. 2005), meaning they are easier to dismiss as unimportant and therefore to ignore (Chao et al. 2014b).

To be common, rare, or absent, is a relative measure (Preston 1948), and relative abundance requires the counting of everything to make such conclusions. Biodiversity is complex and exists on a continuum in multiple dimensions that consequently cannot be comprehensively summarized by a single number (Purvis and Hector 2000; Colwell 2009; Reich et al. 2012) or straightforward categories of when a species is deemed sufficiently common to make a detectable impact on its community. Presenting diversity in integrated ways is an ideal solution (Ellison 2010). Such methods have been applied: effective numbers, or Hill numbers (Hill 1973), integrate richness, evenness, and dominance in one encompassing image (Fig. 1). A drawback of effective numbers is the need for large samples of individuals. To this end, effective numbers have been applied to a range of modern-day taxonomic groups, including tropical ants (Chao et al. 2014b), spiders (Chao et al. 2014b, 2020), corals (Chao et al. 2020), and bacteria (Kang et al. 2016). In the fossil record, assemblages are at the mercy of time and preservation (Jackson and Blois 2015). Therefore, abundant taxa in deep-time samples may not represent true abundance but rather a taphonomically biased sample. Despite these challenges, effective numbers have been applied meaningfully to paleoecological questions focused in the Quaternary investigating the climate and anthropogenic impacts on diversity in shallow-marine ostracods (Hong et al. 2021), deep-sea ostracods (Yasuhara et al. 2016), and pelagic planktonic foraminifera (Yasuhara et al. 2020), as well as Paleozoic marine radiations (Rasmussen et al. 2019).

Conceptually, Hill numbers are the effective number of equally abundant taxa required to give the same diversity presented in the sample (Hill 1973; Jost 2010a; Chao et al. 2014b, 2020). While Hill numbers, like traditional indices such as Shannon's index (H_S) and Simpson's index (H_{GS}), can be presented as single numbers, they normally present diversity (D; Fig. 1) as a function of q, which determines how rare taxa are weighted in relation to abundant taxa (Fig. 1). Therefore, the best representation of Hill numbers is as a function of q. In uneven assemblages, this line is typically a

https://doi.org/10.1017/pab.2022.24 Published online by Cambridge University Press

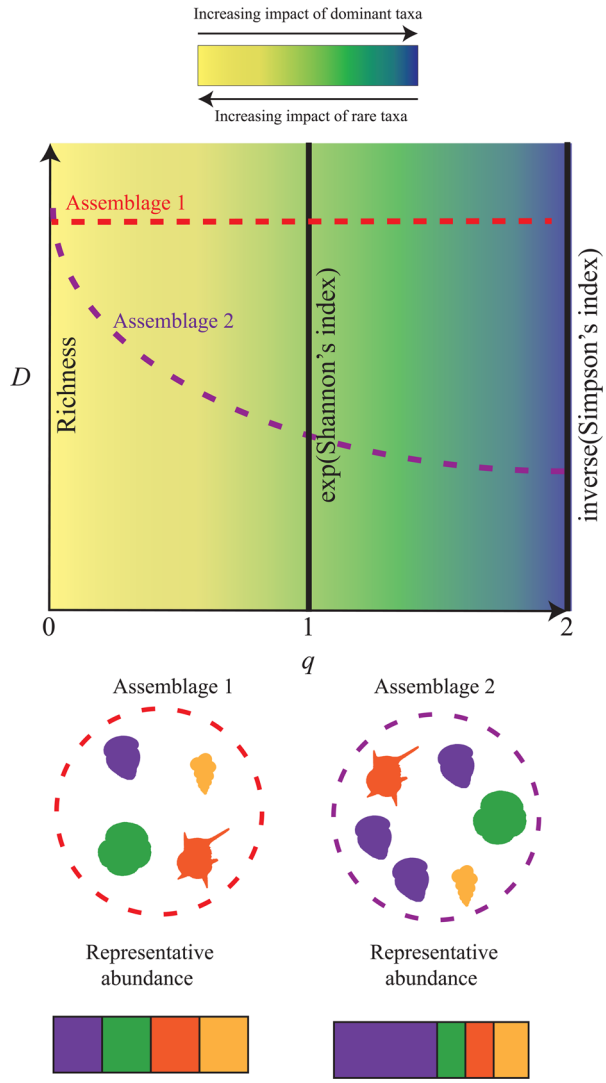

FIGURE 1. Schematic representation of Hill numbers and how q is related to D. The color gradient in the top panel represents the weight given to abundance, with greater weight given as you move to the right. The simplified relationship between diversity line shape and the underlying assemblage is shown. Each colored dashed line is generated from an assemblage containing four taxa. The components of Assemblage 1 are represented equally within the assemblage, so the resulting diversity line is horizontal. The y-intercept is the same for both assemblages, as they have the same number of taxa (four), but Assemblage 2 has a steep gradient, as the purple taxon is more abundant than the green, red, or orange taxa. The silhouettes represent typical planktonic foraminifera of our study interval.

nonlinear curve (Fig. 1) that links the three traditional indices in one image. In addition to being an integrative measure of diversity, Hill numbers also obey the replication principle (Hill 1973). The replication principle is the requirement that when two equal assemblages with no shared taxa and equivalent relative abundances are combined, the diversity of the pooled assemblage is doubled (Hill 1973; Chiu and Chao 2014). This fundamental principle is not obeyed in entropy measures such as Shannon's index. The replicable nature of Hill numbers makes them suitable for detecting diversity changes as a result of environmental perturbations whether they be anthropogenic such as oil spills (McClain et al. 2019; Miller et al. 2020; Heritier-Robbins et al. 2021) or, as in the present study, geologically transient

https://doi.org/10.1017/pab.2022.24 Published online by Cambridge University Press

climatic events. The commonality of units at all levels of q means that inferences can be made regarding magnitudes of change (Jost 2007, 2010a; Chao et al. 2014b) and sample and locality differences (Hill 1973; Chao et al. 2014a) and enables the transformation to commonly used general entropy metrics such as Shannon's index and Simpson's index. In addition, Hill numbers can be applied to other aspects of diversity such as phylogenetic (Chao et al. 2010), functional (Chiu and Chao 2014), and taxonomic (Chao et al. 2014a) diversity, with straightforward bootstrapping techniques to quantify how high proportions of singletons increase uncertainty (Chao et al. 2014a).

To be meaningful, Hill number calculations require sufficient and careful sampling protocols. Here we calculate Hill numbers for a deep-time community, outlining best practices for sample analysis by tracking planktonic foraminiferal diversity changes across the middle Eocene climatic optimum (MECO), ~40 Ma (Bohaty and Zachos 2003; Bohaty et al. 2009; Rivero-Cuesta et al. 2019; Edgar et al. 2020). The requirement for large samples of individuals means fossilized planktonic foraminifera are an ideal candidate for Hill numbers (Yasuhara et al. 2020) as a result of their readily preserved calcium carbonate tests. In the modern oceans, planktonic foraminifera are represented by ~50 species and ~24 genera (Schiebel and Hemleben 2001; Kucera 2007; Brummer and Kučera 2022), which upon death are deposited on the seafloor in vast quantities, producing ~2 Gt of calcite per year (Schiebel and Hemleben 2008). Deposition of planktonic foraminifera has occurred nearly continuously since their evolution ~200 Ma during the Jurassic period (Fraass et al. 2015), and foraminifera-rich sediments have been recovered around the globe by the coring efforts of the International Ocean Discovery Program (IODP) and its predecessors. Because planktonic foraminiferal diversity shows a strong affinity to climatic fluctuations (Ezard et al. 2011; Fraass et al. 2015; Fenton et al. 2016a; Yasuhara et al. 2017) with a highly temporally and spatially resolved record (Fenton et al. 2021), this is an ideal study system to investigate ecosystem responses to transient and rapid climatic perturbations.

Here we apply Hill numbers to understand planktonic foraminifera community response through the MECO. The middle to late Eocene encapsulates the long-term cooling from the Eocene "hothouse" of the early Eocene climatic optimum (EECO, 53–48 Ma; Westerhold et al. 2018, 2020) through to the "icehouse" of the Oligocene that started at the Eocene/Oligocene transition (EOT, 34 Ma; Westerhold et al. 2020; Hutchinson et al. 2021) with the establishment of continent-wide Antarctic glaciation (Zachos et al. 1996; Coxall et al. 2005). The cooling trend in global temperature through this interval was interrupted by a transient (~270–500 kyr) warming event between ~40.6 and 40 Ma known as the MECO (Bohaty and Zachos 2003; Bohaty et al. 2009; Rivero-Cuesta et al. 2019). During the MECO, there was a transient ~3°C–6°C rise in surface and deep-water temperatures (Bohaty and Zachos 2003; Bohaty et al. 2009; Bijl et al. 2010; Galazzo et al. 2014; Cramwinckel et al. 2019; Henehan et al. 2020), reduced surface ocean pH (Henehan et al. 2020), and a shoaling of the calcium carbonate compensation depth (CCD; Bohaty and Zachos 2003; Bohaty et al. 2009). The MECO is terminated by a rapid return to pre-MECO conditions (Bohaty et al. 2009) and the continuation of the long-term cooling trend from the Eocene hothouse to the Oligocene icehouse.

In conjunction with the Eocene climate transition from greenhouse to icehouse conditions, there were also profound changes in planktonic foraminiferal diversity (Steineck 1971; Boersma and Premoli Silva 1986; Boersma and Silva 1991; Keller et al. 1992; Wade 2004; Sexton et al. 2006; Wade and Pearson 2008; Luciani et al. 2010; Ezard et al. 2011; Galazzo et al. 2014; Fenton et al. 2016a). Middle Eocene biotic changes in planktonic foraminifera include: (1) the progressive extinction of surface-dwelling, symbiont-bearing taxa (Boersma and Premoli Silva 1986; Boersma and Silva 1991; Keller et al. 1992; Wade 2004; Wade and Pearson 2008); (2) a reduction in test size (Schmidt et al. 2004; Wade and Pearson 2008; Wade and Olsson 2009); (3) development of latitudinal size (Schmidt et al. 2004) and diversity (Fenton et al. 2016a) gradients alongside major assemblage fluctuations (Steineck 1971; Keller 1983; Boersma and Premoli Silva 1986;

https://doi.org/10.1017/pab.2022.24 Published online by Cambridge University Press

Boersma et al. 1987; Hallock et al. 1991; Keller et al. 1992; Sexton et al. 2006; Luciani et al. 2010; Galazzo et al. 2014); and (4) changes in ecology, for example, loss or inhibition of algal photosymbionts from hosting taxa (Wade et al. 2008; Edgar et al. 2013) and shallowing depth habitat of *Hantkenina* (Coxall et al. 2000). Yet our understanding of planktonic foraminifera ecosystem dynamics across the MECO remain relatively understudied compared with other periods of the Eocene such as the EOT (e.g., Pearson et al. 2008; Wade and Pearson 2008; Pearson and Wade 2015). The MECO resulted in a global crisis for muricate taxa (Luciani et al. 2010; Edgar et al. 2013), varying symbiotic taxon responses (Luciani et al. 2010; Edgar et al. 2013; Gebhardt et al. 2013; Arimoto et al. 2020; Kearns et al. 2021), and increased abundance of ecologically flexible (Galazzo et al. 2015; Kearns et al. 2021) and small opportunistic taxa (Luciani et al. 2010). What we lack, however, is an integrated assemblage perspective on these idiosyncratic changes, pieced together from different sampling localities. Here, using Hill numbers, we generate the first midlatitude diversity record of planktonic foraminifera at North Atlantic sites through the MECO to investigate how planktonic foraminifera communities responded to the MECO and how this event may have influenced subsequent extinction events observed in the late Eocene. Furthermore, we analyze diversity within two size fractions (>63 μm and >180 μm) to understand the effects of sampling bias on diversity and its implications for our understanding of biotic responses to climatic perturbations.

Materials and Methods

Materials

IODP Expedition 342 targeted clay-rich Paleogene sediment drifts ~700 km east-southeast of Newfoundland in the northwest Atlantic Ocean (Norris et al. 2014), which were deposited at a paleolatitude of ~32.5°N (Supplementary Fig. 1). Expedition 342 Sites U1406 (40°21.0′N, 51°39.0′W; modern water depth: ~3814 m), U1408 (41°26.3′N, 49°47.1′W; modern water depth: ~3022 m), and U1410 (41°19.6993′N, 49°10.1847′W; modern water depth: ~3387 m) recovered clay-rich nannofossil ooze drift deposits well above the late Paleogene CCD, providing near-continuous records of well-preserved microfossils from ~47 Ma through the Eocene and into the Oligocene (Norris et al. 2014; Boyle et al. 2017). Using low-resolution bulk stable isotope data (S. M. Bohaty unpublished data) as a guide, cores from Sites U1406, U1408, and U1410 were sampled to capture a 7 Myr interval of the middle Eocene spanning the MECO. In total, 33 samples of 25 cc between 38 and 45 Ma were studied. Due to changes in sediment accumulation rates during parts of the MECO, sampling resolution ranges from ~20 kyr during the MECO to ~900 kyr outside the MECO.

Sample ages from Sites U1408 and U1410 were calculated based on age–depth models constructed using available biostratigraphy and magnetostratigraphy (Norris et al. 2014). The 2012 geological timescale was then used for age calibrations for the middle Eocene geomagnetic reversals (GTS2012; Gradstein et al. 2012). Sample ages for Site U1406 are based upon shipboard biostratigraphic and magnetostratigraphic data (Norris et al. 2014; Van Peer 2017). Sample information, including calculated ages, is presented in Supplementary Table 1.

Sample Preparation

The sample material was disaggregated in a sodium hexametaphosphate solution and then washed over a 38 μm sieve with milli-Q water until the water ran clear. Following 24 hours of drying in a low-temperature oven (<50°C), samples were weighed to determine the weight percent coarse fraction (>38 μm). Subsequently, each sample was split, using a microsplitter, providing two representative halves: one for diversity analysis (this study) and the other for geochemical analysis (Kearns et al. 2021). The half reserved for diversity analysis in this study was then split again to allow analyses at two different size fractions. Planktonic foraminiferal assemblage studies typically only analyze size fractions >150 μm (Kucera et al. 2005) to avoid sampling juvenile specimens and to enable species-level identification (Al-Sabouni et al. 2007, 2018). This, by definition, biases assemblages toward larger forms, despite suggestions that analyzing a >63 μm size fraction, especially

https://doi.org/10.1017/pab.2022.24 Published online by Cambridge University Press

in polar regions where species are generally smaller, is more representative of true diversity (Al-Sabouni et al. 2007). To test whether a smaller size fraction is more characteristic of diversity at midlatitude, nonpolar sites like IODP Expedition 342, we determined diversity in two size fractions: >63 μm and >180 μm. To avoid juveniles in the smaller size fractions, only individuals showing adult characteristics related to aperture position, keels, and fully developed pore structure in macroperforate forms were picked for analysis (Brummer et al. 1986).

Diversity Analysis

A sample of 300 individuals is considered sufficient to estimate diversity in foraminiferal assemblages (Al-Sabouni et al. 2007), despite the potential for missing rare specimens due to low abundances (Jost 2010b). For this study, each sample in both size fractions (>63 μm and >180 μm) was further split using a microsplitter until approximately 300 individuals were present on the picking tray, with a minimum cutoff of 200 specimens. All individuals in the subsample were then picked to avoid bias as a result of uneven distribution on the tray and identified to the genus level (Supplementary Tables 2–4) based on published taxonomy (Pearson et al. 2006; Wade et al. 2018).

To understand diversity changes further, we then classified all genera into morphogroups (Supplementary Tables 5, 6) adapted from previous classifications (Aze et al. 2011) and depth habitats (Supplementary Tables 7, 8). We based morphogroup classifications on morphological traits (Supplementary Table 9) and depth habitats (Supplementary Table 10) on published ecological inferences obtained from stable isotope measurements (summarized in Pearson et al. 2006; Wade et al. 2018). Relative abundances and effective diversity curves were than calculated for each genus, morphogroup, and ecogroup.

We calculate diversity as a curve using Hill numbers (Hill 1973):

$$ {}^{q}D = \left(\sum_{i=1}^{S} p_i^q \right)^{1/(1-q)} \quad (1) $$

where S is the number of taxa and p_i the frequency of the ith taxa. The value of D is dependent on the order, q, which determines how rarity is weighted in relation to abundance. At $q = 0$, taxic richness is measured such that abundance is ignored, as rare taxa are weighted more heavily than common taxa compared with higher powers of q (Fig. 1). As q gets larger, the weighting toward rare taxa is reduced and relative abundance is considered. At $q = 1$, rare and common taxa are equally weighted, which equates to the exponential of Shannon's index (Chao and Jost 2012; Fig. 1). At $q = 2$, only relative abundance is accounted for, removing the influence of rare taxa, so this measure is equivalent to the inverse of Simpson's index (Chao and Jost 2012; Fig. 1). While these integer values are useful reference points, the strength of the Hill number approach is how the continuum of q values (the slope of the effective diversity curve) can be used to understand the evenness of the assemblage. If an assemblage is made up of equal numbers of represented taxa, then the diversity curve will be flat, as abundance does not vary among between groups and no taxon is rare (Fig. 1). In contrast, if the curve has a high gradient and plummets into a plateau, then the assemblage can be interpreted as uneven with lots of rare taxa and a few dominant groups (Fig. 1).

We outline the workflow for calculating our diversity curves, which follows Chao and Jost (2015), in the Supplementary Material. Effective diversity was calculated at the default 0.1 intervals for q between 0 and 2 (Chao and Jost 2015; Supplementary Table 11). Confidence intervals were generated at the 95% level for each diversity curve by bootstrapping 1000 times.

Fragmentation

A challenge to using paleoecological data is the inevitable influence of taphonomic bias. Assemblage data of planktonic foraminifera can be heavily influenced by the physiochemical process of dissolution as a result of their shell (test) composition (Berger 1971; Malmgren 1987; Nguyen et al. 2009). The susceptibility of foraminifera to dissolution is strongly species specific based on the physical structure of the test wall (e.g., relative porosity and

https://doi.org/10.1017/pab.2022.24 Published online by Cambridge University Press

thickness; Nguyen et al. 2009, 2011; Nguyen and Speijer 2014) and is influenced by the microenvironment of the individual, which influences test chemistry and causes interspecific differences in dissolution susceptibility (Berger 1970; Nguyen et al. 2011; Petro et al. 2018). To account for this variability, we use an accepted fragmentation proxy to estimate the dissolution levels (Le and Shackleton 1992), using the proportion of planktonic foraminiferal test fragments (Frag) and whole specimens:

$$\text{Fragmentation (\%)} = (\text{Frag}/8)/(\text{Frag}/8 + \text{Whole}) \times 100 \quad (2)$$

We classify a fragment as anything <75% of a whole specimen (which is more conservative than the <50% previously used; Malmgren 1987). Foraminifera have a tendency to break into multiple pieces; therefore, the percentage of fragments in a sample varies nonlinearly with dissolution (Le and Shackleton 1992). To account for this, a divisor is used to represent the average number of pieces a foraminifera breaks into, and we follow previous work and set the divisor as 8 (Le and Shackleton 1992; Leon-Rodriguez and Dickens 2010). We use a baseline of 20% fragmentation to indicate normal levels of fragmentation and dissolution (Pfuhl and Shackleton 2004). Samples sieved at 63 μm are expected to have higher fragmentation than samples sieved at a larger size fraction, as fragments progressively break into smaller pieces and smaller individuals are less robust. Therefore, we use the percentage of coarse fraction after sieving to assess potential dissolution effects on the assemblage, as dissolution reduces the absolute abundance of planktonic foraminifera in a sample while ecological change causes taxon relative abundance fluctuations. Fragmentation was calculated twice on 18 samples (9 samples from the >180 μm fraction and 9 samples from the >63 μm fraction) with high repeatability (92%; Supplementary Table 12).

Statistical Methods

Generalized Additive Models.—Diversity has a nonlinear relationship with time. To assess the impact of sample age and size fraction on diversity, we applied nonparametric generalized additive models (GAMs) using the R package mgcv (v. 1.8.33; Wood 2017) in the R environment (v. 4.0.3; R Core Team 2020). Before model fitting, integer values of Hill numbers were back transformed to genus richness, Shannon's index (H_S), and Simpson's index (H_{GS}) and used as response variables. Models were constructed with a smooth (nonparametric, nonlinear) function of age and a linear predictor of fragmentation to control for the impact on dissolution on diversity. Models were fit using a Gaussian distribution with an identity link using a generalized cross-validation model (GCV) method. A GCV method was used instead of restricted maximum-likelihood estimation (REML) due to the small number of samples through time (Wood 2011). The code to obtain predictions based on observed and defined fragmentation can be found in the Supplementary Material.

Model selection among a relevant model set including a null model (Table 1) was based on Akaike information criterion corrected for small sample size (AICc) and diagnostic plots. The Supplementary Material provides further detail on back transformation, models fit (including all annotated code), and model selection information. Model results relating to significance of smoothing parameters are presented with effective degrees of freedom (edf), *F*-statistics (F), and *p*-values (p). The edf indicates the complexity of the curve; an edf of 1 indicates a straight line, while an edf of 2 indicates a quadratic curve, and so on. In addition, where appropriate, parametric coefficients are presented with the coefficient (β), *t*-value (t), standard error (SE), and *p*-value (p).

Kruskal-Wallis and Dunn Tests.—To investigate differences in Hill numbers in response to paleoclimatic and paleoceanographic changes, samples were divided into three time slices representing different climate phases (pre-MECO: >41.94 Ma; MECO: 41.09–40.14 Ma; post-MECO: <40.14 Ma). The difference between these intervals was assessed when q <1 (weighted toward rarity) and q >1 (relative abundance taken into account) using a Kruskal-Wallis test. A Kruskal-Wallis test was used to investigate whether a difference was present

https://doi.org/10.1017/pab.2022.24 Published online by Cambridge University Press

TABLE 1. Table showing the structure of all models fit. Diversity is replaced by genus and morphogroup for each set of models, and Akaike information criterion (AIC) weights are presented. The smooth term is denoted by s().*Best-fitting model. †Null model. All other statistical output, including df and AIC, is provided in Supplementary Tables 13–18.

	Generic AIC weight			Morphogroup AIC weight		
Model structure	Richness	Shannon's index	Simpson's index	Richness	Shannon's index	Simpson's index
Diversity ~ s(Age, by = size) + size + Frag*	0.9959	1.0000	1.0000	0.9999	1.0000	1.0000
Diversity ~ s(Age, by = size) + Frag	0.0002	0.0000	0.0000	0.0000	0.0000	0.0000
Diversity ~ s(Age) + Frag	0.0010	0.0000	0.0000	0.0000	0.0000	0.0000
Diversity ~ s(Age)†	0.0030	0.0000	0.0000	0.0000	0.0000	0.0000

between intervals, and additionally the effect size of the intervals was calculated based on the H statistic from the Kruskal-Wallis test. Following detection of a statistically significant impact of interval in the Kruskal-Wallis test ($p < 0.01$), a post hoc Dunn test using the R package "FIA" (Ogle et al. 2022) was applied, due to unequal observations in each interval (Zar 2010), to identify intervals which were significantly different from each other.

Results

Fragmentation

The degree of fragmentation varies across our record from 1.34% to 30.80% (Supplementary Fig. 2, Supplementary Table 11), with generally increased fragmentation in the smaller size fraction, as expected. In total, seven samples were above the baseline "normal" fragmentation of 20% (Pfuhl and Shackleton 2004), of which six were in the >63 μm size fraction. These were primarily within the MECO interval (~41–40 Ma) and at ~38 Ma.

Traditional Diversity Indices

In total 18 genera consisting of 11 morphogroups occupying three depth habitats were identified (Supplementary Table 2). On average, samples consisted of 11 and 9 genera in the >63 μm and >180 size fractions, respectively (Supplementary Tables 3, 4). In the >63 μm fraction, only three genera were present in all 33 samples (*Subbotina*, *Acarinina*, and *Planorotalites*; Supplementary Table 3), while in the >180 μm size fraction, only *Subbotina* was found in all samples (Supplementary Table 4). This study is based on genera, for reasons outlined in the "Introduction"; however, we note that all genera were represented by approximately two or fewer species, except for *Subbotina*, which was represented by approximately six species.

Integers of effective diversity are equivalent to transformed versions of common diversity measures (genus richness [$q = 0$], Shannon's index (H_S) [$q = 1$], and Simpson's index (H_{GS}) [$q = 2$]). To understand how commonly used diversity indices changed through time and aid comparison with other studies, we back-transformed calculated Hill numbers into genus richness, H_S and H_{GS} indices for genera, morphogroup, and ecogroup, and fitted GAMs (Fig. 2, Table 1). For all diversity indices, based on AICc, the best-fitting GAMs (Tables 1, 2, Supplementary Tables 13–21, Supplementary Figs. 3–11) suggest a change in diversity as a function of size fraction, with varying intercepts for size fraction (with the smaller size fraction giving consistently higher values), during the Eocene for richness, H_S, and H_{GS}. We concentrate here on generic and morphogroup changes in terms of richness, H_S, and H_{GS} (depth-habitat effects on diversity changes are discussed in "Hill Numbers and Relative Abundance Fluctuations"). Depth-habitat analysis showed similar patterns, but with only three depth groups, the changes observed were non-consequential in terms of H_S and H_{GS} and are therefore provided in Supplementary Figs. 9–12 and Supplementary Tables 21–23. The ΔAICc between the best-fitting models for genera and morphogroup and the next best models ranged from 11.595 to 71.331 (Supplementary Tables 14–18), implying that the second-ranked models had "essentially no" support (Burnham and Anderson 2002).

Following model selection, we used the best-fitting model (Tables 1, 2) to predict diversity values across our study interval at a mean fragmentation of 10% based on the mean of our

https://doi.org/10.1017/pab.2022.24 Published online by Cambridge University Press

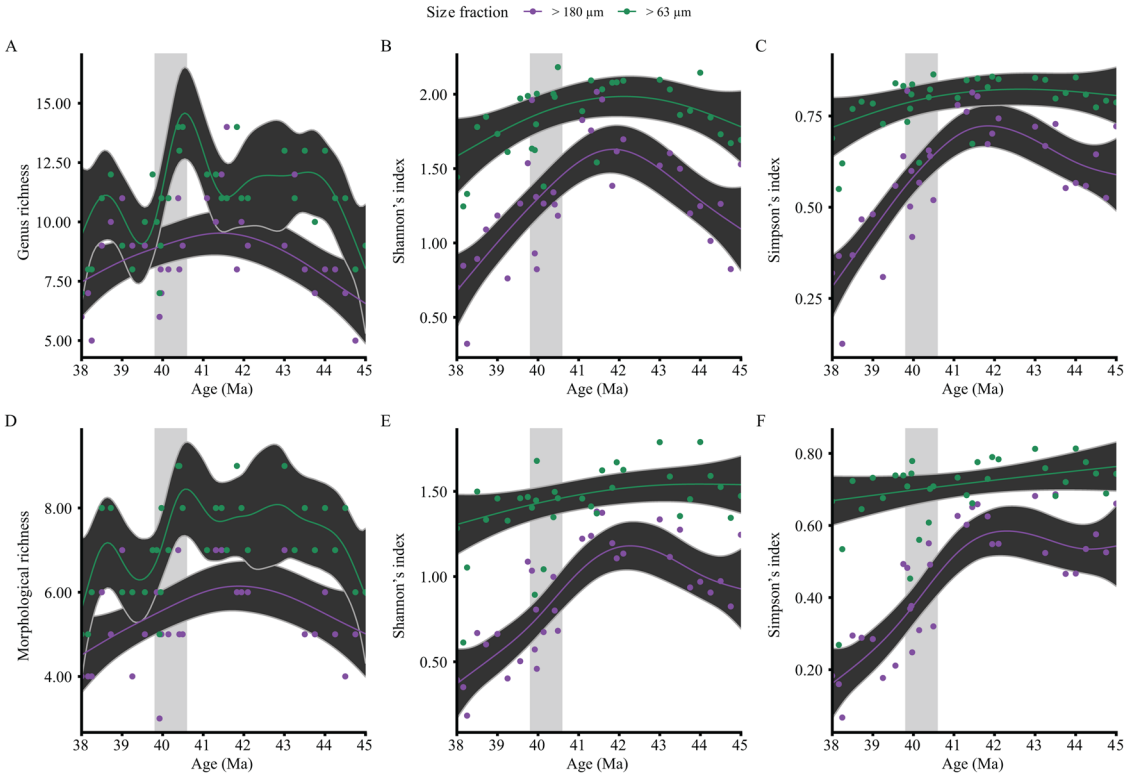

FIGURE 2. North Atlantic predicted diversity from International Ocean Discovery Program (IODP) Expedition 342 (Sites U1406, U1408, and U1410) as a function of time at >63 µm (green) and >180 µm (purple) size fractions. Note that these predictions control for fragmentation, which we assume in this prediction to be 10% (the mean fragmentation of our samples). Raw data are shown as filled circles. Black shaded area represents 95% confidence intervals around the central predicted response. A–C show generic diversity indices; D–F show morphological diversity indices. The light gray box represents the middle Eocene climatic optimum (MECO) interval.

TABLE 2. Table showing the parametric coefficients for best-fitting generalized additive models (GAMs) shown in Table 1 based on Akaike information criterion (AIC) difference compared with next best fitting model being more than 2. Frag, fragmentation; size, size fraction (>63 µm or >180 µm).

Model	*q*	Parametric coefficient	Estimate	SE	*t*-value	*p*-value
Genera ~ s(Age, by = size) + size + Frag	0	Intercept	12.4	0.63	19.8	0
Genera ~ s(Age, by = size) + size + Frag	0	Size:180	−2.64	0.46	−5.75	0
Genera ~ s(Age, by = size) + size + Frag	0	Fragmentation	−0.12	0.04	−2.91	0.01
Genera ~ s(Age, by = size) + size + Frag	1	Intercept	1.93	0.08	23.56	0
Genera ~ s(Age, by = size) + size + Frag	1	Size:180	−0.58	0.07	−8.75	0
Genera ~ s(Age, by = size) + size + Frag	1	Fragmentation	−0.01	0.01	−1.4	0.17
Genera ~ s(Age, by = size) + size + Frag	2	Intercept	1.68	0.09	19.09	0
Genera ~ s(Age, by = size) + size + Frag	2	Size:180	−0.67	0.07	−9.42	0
Genera ~ s(Age, by = size) + size + Frag	2	Fragmentation	−0.01	0.01	−1.2	0.23
Morphogroup ~ s(Age, by = size) + size + Frag	0	Intercept	7.49	0.37	20.04	0
Morphogroup ~ s(Age, by = size) + size + Frag	0	Size:180	−1.73	0.28	−6.23	0
Morphogroup ~ s(Age, by = size) + size + Frag	0	Fragmentation	−0.03	0.03	−1.02	0.31
Morphogroup ~ s(Age, by = size) + size + Frag	1	Intercept	1.57	0.06	24.56	0
Morphogroup ~ s(Age, by = size) + size + Frag	1	Size:180	−0.61	0.05	−11.61	0
Morphogroup ~ s(Age, by = size) + size + Frag	1	Fragmentation	−0.01	0	−2.74	0.01
Morphogroup ~ s(Age, by = size) + size + Frag	2	Intercept	0.77	0.03	25.96	0
Morphogroup ~ s(Age, by = size) + size + Frag	2	Size:180	−0.28	0.02	−11.62	0
Morphogroup ~ s(Age, by = size) + size + Frag	2	Fragmentation	−0.01	0	−3.07	0

https://doi.org/10.1017/pab.2022.24 Published online by Cambridge University Press

fragmentation counts (10.37%; Supplementary Fig. 2, Supplementary Table 11) to produce diversity curves and 95% confidence intervals (Fig. 2). For completeness, model predictions were also done at 5% and 20% fragmentation, which resulted in no change in predicted diversity values.

Richness.—Spline complexity ("wigglyness") for genera differed between size fractions, with a more complex spline predicted for the >63 µm size fraction (edf = 8.54, $F = 3.10$, $p < 0.01$) compared with the >180 µm size fraction (edf = 2.65, $F = 4.27$, $p < 0.01$) (Fig. 2A). A similar pattern was observed in the morphogroup models, where the predicted spline for >63 µm size fraction is more complex (edf = 8.26, $F = 2.16$, $p < 0.05$) than the >180 µm size fraction (edf = 2.38, $F = 3.10$, $p < 0.05$) (Fig. 2D). The complex nature of the >63 µm size fraction spline illustrates intersample variability represented in the larger confidence intervals compared with the >180 µm size fraction (Fig. 2A,D).

Morphological and generic richness profiles generally follow a similar pattern, with increasing richness initially between 45 and 44 Ma, followed by a period of relative stasis until ~41.5 Ma (Fig. 2A,D). In the >63 µm size fraction, generic and morphological richness peaked at ~40.55 Ma, coinciding with the early stages of the MECO (generic: 14.71 ± 0.98, morphological: 8.45 ± 0.55; Fig 2A,D). In the >180 µm size fraction, the peak in richness is much less pronounced and occurs ~1 Myr before the MECO at 41.54 Ma (generic: 9.52 ± 0.47; Fig. 2A) and 41.89 Ma (morphological: 6.14 ± 0.30; Fig. 2D). Peaks in morphological and generic richness in the >180 µm size fraction are followed by a decline of a mean of 1.64 morphogroups and 2.06 genera by the end of our record at 38.00 Ma (Fig. 2A,D). The wide 95% confidence intervals around the richness declines (Fig. 2A,D) suggest no detectable fall, as the confidence intervals could encapsulate a straight horizontal line. In contrast, the >63 µm size fraction shows a greater degree of intrasample variability resulting in more complex GAMs that predict a large decline in morphological (−2.17 morphogroups) and generic (−5.62 genera) richness following the MECO at ~40.5 Ma (Fig. 2A,D).

The most influential predictor of generic and morphological richness was size, with a predicted reduction in overall richness of 2.537 genera ($\beta = -2.537$, SE = 0.468, $t = -5.423$, $p < 0.001$) and 1.728 morphogroups ($\beta = -1.728$ SE = 0.277, $t = -6.235$, $p < 0.001$), calculated through analysis assemblages from the >180 µm size fraction rather than >63 µm size fraction (Table 2). This means that 2.537 genera and 1.728 morphogroups represented in the >63 µm size fraction are not present in the >180 µm size fraction. Fragmentation was also a significant predictor for generic richness with a predicted 0.14 decrease in richness per 1% increase in fragmentation ($\beta = -0.14$, SE = 0.048, $t = -13.16$, $p < 0.001$; Table 2).

Shannon's Index.—The predicted curves for H_S are smoother than those for richness (Fig. 2). However, unlike richness, the model predicted a more complex age spline for generic H_S in the >180 µm size fraction (edf = 3.06, $F = 11.65$, $p < 0.001$) than in the >63 µm size fraction (edf = 2.18, $F = 2.73$, $p > 0.05$; Fig. 2B, Supplementary Table 20). Among genera, size is the only significant predictor of diversity ($\beta = -0.58$, SE = 0.10, $t = -8.68$, $p < 0.001$; Supplementary Table 20), with the >180 µm size fraction predicted to increase to a peak of 1.64 ± 0.08 at 41.89 Ma followed by a steep decline until 38.00 Ma (Fig. 2B). In contrast, the >63 µm size fraction gradually increases, reaching a maximum H_S of 1.99 ± 0.07 at 42.10 Ma (Fig. 2B).

For morphological H_S, the age spline for the >63 µm fraction does not differ detectably from a straight line (edf = 1.62, $F = 2.28$, $p > 0.05$; Supplementary Table 20), in contrast to the wiggly spline for >180 µm (edf = 3.47, $F = 13.67$, $p < 0.001$; Fig. 2E, Supplementary Table 20). Both fragmentation and size fraction are significant predictors (fragmentation: $\beta = -0.011$, SE = 0.004, $t = -2.74$, $p < 0.01$; size fraction: $\beta = -0.61$, SE = 0.05, $t = -11.61$, $p < 0.001$; Table 2), but size fraction has a larger, more meaningful impact on diversity, with a reduction of 0.61 morphogroups in the >180 µm size fraction compared with the >63 µm size fraction. The peak in >180 µm morphological H_S (1.18 ± 0.07) is predicted at 42.40 Ma, 0.50 Ma before the peak in generic H_S in the same size fraction (Fig. 2B,E).

Simpson's Index.—Through the narrow range of values allowed for available values

https://doi.org/10.1017/pab.2022.24 Published online by Cambridge University Press

for H_{GS} (between 0 and 1), intersample variation was high (Fig. 2 C,F), and the predicted spline follows a pattern similar to that in H_S (Fig. 2). The GAMs predicted a complex age spline for genera (edf = 3.31, $F = 19.11$, $p < 0.001$; Supplementary Table 20) and morphogroup (edf = 3.64, $F = 17.94$, $p < 0.001$; Supplementary Table 20) H_{GS} in the >180 μm size fraction. Both splines reach peaks before the MECO at 41.82 Ma (Fig. 2C) and 42.31 Ma (Fig. 2F) for morphogroup and generic H_{GS}, respectively. The age spline for the smaller size fractions is not detectably different from straight lines (genera: edf = 1.88, $F = 2.01$, $p > 0.05$; morphogroup: edf = 1.06, $F = 2.24$, $p > 0.05$; Fig. 2C,E, Supplementary Table 20). In genera, only fragmentation is a significant predictor equating to a predicted 0.21 ± 0.02 reduction in generic Simpson's index per 1% increase in fragmentation (β = −0.21, SE = 0.02, $t = -9.40$, $p < 0.001$; Table 2), while for morphogroup, both fragmentation (β = −0.01, SE = 0.002, $t = -3.06$, $p < 0.01$; Table 2) and size fraction (β = −0.28, SE = 0.02, $t = -11.62$, $p < 0.001$; Table 2) are significant predictors of H_{GS}.

Hill Numbers and Relative Abundance Fluctuations

Genera.—When relative abundance is not considered ($q < 1$), pre-MECO (>41.09 Ma), MECO (41.09–40.14 Ma), and post-MECO (<40.14 Ma) intervals are all different from each other (Fig. 3A,D; $p < 0.001$), but the effect of size ($\eta^2[H] = 0.18$) and magnitude of differences between intervals (pre-MECO, MECO, and post-MECO) is only large (defined in the statistical test as an effect size ($\eta^2[H]$) > 0.14) in the >63 μm size fraction (Supplementary Table 24). This suggests substantial differences in absolute numbers of genera through the middle Eocene, with highest values in the MECO (41.09–40.14 Ma) followed by a decline into post-MECO (<40.14 Ma) assemblages below pre-event levels (Fig. 3A,D).

When relative generic abundance is considered ($q > 1$), the effect size of time interval is only large ($\eta^2[H] = 0.25$) and significant ($p < 0.01$) in the >180 μm size fraction (Supplementary Table 23). A Dunn's test shows that a significant difference exists between the post-MECO interval (<40.14 Ma) and the other intervals ($p < 0.01$; Supplementary Table 24), with the MECO (41.09–40.14 Ma) and pre-MECO interval (>41.09 Ma) showing no significant differences.

Morphogroup.—In the >63 μm size fraction, the effective diversity curves show only subtle separation between assemblages because of paleoceanographic changes (interval) (Fig. 3B). A Kruskal-Wallis test revealed morphological effective diversity was only significantly different ($p < 0.01$) between time intervals, with a large effect size of interval ($\eta^2[H] = 0.25$) when relative abundance was considered ($q > 1$; Fig. 3B, Supplementary Table 24). Based on a Dunn's test, the detectable interval differences are between the MECO (41.09–40.14 Ma) and pre-MECO (>41.09 Ma; $p < 0.05$), as well as between the post-MECO (<40.14 Ma) and pre-MECO (>41.09 Ma; $p < 0.05$; Supplementary Table 25).

In the >180 μm size fraction, the effect size of time interval is clear when rare morphologies are influential ($q < 1$) and when they are discounted ($q = 1$–2) (Supplementary Table 24). A Dunn test showed that there is no detectable difference between pre-MECO and MECO (41.09–40.14 Ma) samples ($p > 0.1$) at any level of q (Supplementary Table 25), resulting in overlapping effective diversity curves, except for those assemblages grouped in the post-MECO (<40.14 Ma) assemblages colored purple (Fig. 3E). Additionally, the post-MECO (<40.14 Ma) assemblages show a decrease in evenness compared with the preceding intervals (Fig. 3E).

Depth Habitat.—Compared with the generic and morphogroup analyses, effective depth-habitat richness ($q = 0$) in assemblages is the same in both size fractions (3; Fig. 3C,F), with no differences in depth habitat as a function of size fraction or sample age. A Kruskal-Wallis test showed no difference in effective diversity between paleoceanographic intervals in the >63 μm size fraction, which is illustrated by the overlap of effective diversity curves (Fig. 3C). This implies that there was no change in depth-habitat evenness through the middle Eocene, meaning no organisms of a certain depth habitat were dominating assemblages.

In comparison, the depth-habitat effective number curves show separation in the post-MECO (<40.14 Ma) samples of the >180 μm

https://doi.org/10.1017/pab.2022.24 Published online by Cambridge University Press

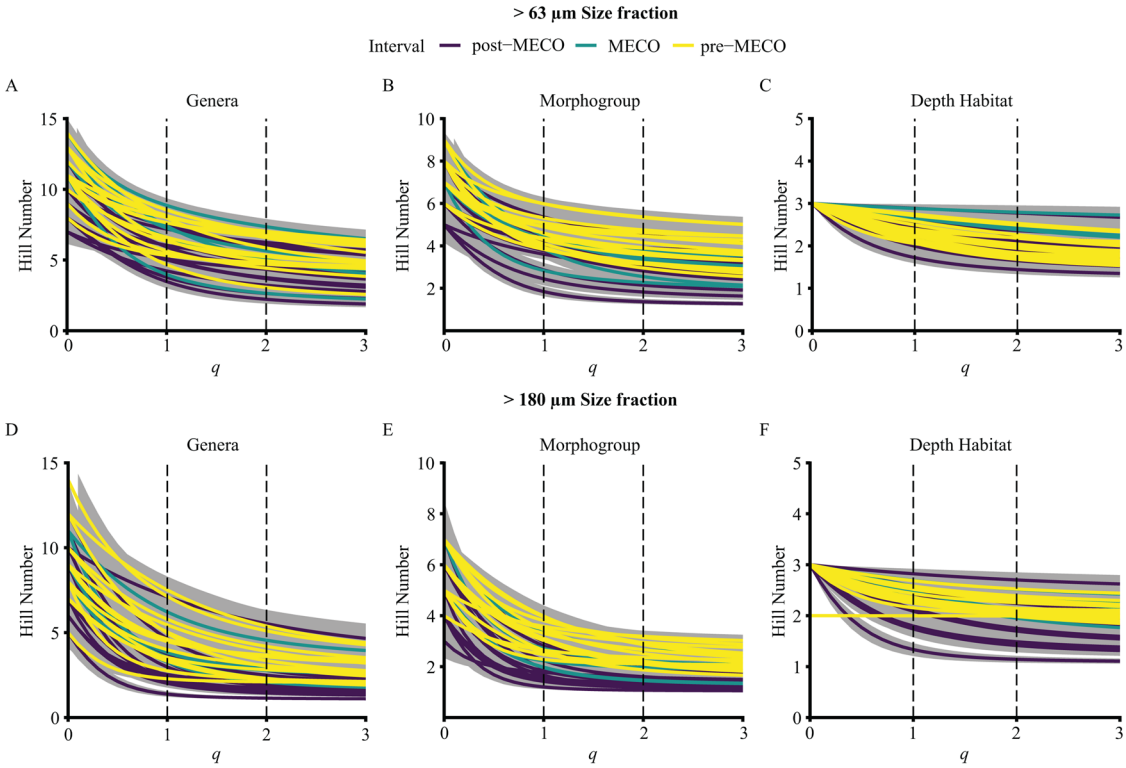

FIGURE 3. North Atlantic diversity curves showing Hill number calculations based on abundance counts presented in Supplementary Tables 3 and 4. Morphogroup and depth habitat follow the classification outlined in Supplementary Tables 9 and 10. A–C reflect diversity changes at the >63 µm size fraction, while D–F reflect changes at the >180 µm size fraction. All panels show a reduction in evenness in post–middle Eocene climatic optimum (post-MECO) communities compared with pre-MECO and MECO assemblages. D–F, The larger size fraction has steeper curves, reiterating the potential dangers of unrepresentative community sampling. Vertical dotted lines are present where $q = 1$ and $q = 2$, as these correlate to the exponential of Shannon's index ($q = 1$) and the inverse of Simpson's index ($q = 2$) presented in Fig. 2. Lines are colored to represent paleoceanographic intervals. Note one horizontal yellow line in F illustrating a perfectly even assemblage. The gray bands represent 95% confidence intervals.

size fraction (Fig. 3F). A Kruskal-Wallis test showed that the interval had a large effect size ($\eta^2[H] = 0.262$) with a clear impact ($p < 0.01$) when q is between 1 and 2 in the >180 µm size fraction (Supplementary Table 24). A Dunn test show that the detectable differences are between the post-MECO (<40.14 Ma) interval and both preceding intervals ($p < 0.01$; Supplementary Table 25). The gradient change of the effective diversity curves also shows that the post-MECO (<40.14 Ma) samples are uneven compared with the other intervals.

Discussion

Understanding biodiversity responses to climate change is challenging, particularly in deep time. A focus on relative abundance changes and biogeographic comparisons can complicate broader interpretations because of the idiosyncratic responses of taxa to environmental change. By using Hill numbers, we have been able to generalize and assess the biodiversity response of planktonic foraminifera temporally to transient warming (Fig. 3) at mid-latitudes, while maintaining the ability to investigate more specific biodiversity measures such as richness (Fig. 2) and relative abundance changes (Fig. 4).

Using this approach, we show increases in morphological and generic richness coincident with the early and middle stages of MECO warming in the >63 µm size fraction (Fig. 2A, D), which is reflected in our count data with ~70% of all genera and morphogroups we found present at ~40.5 Ma (Supplementary

https://doi.org/10.1017/pab.2022.24 Published online by Cambridge University Press

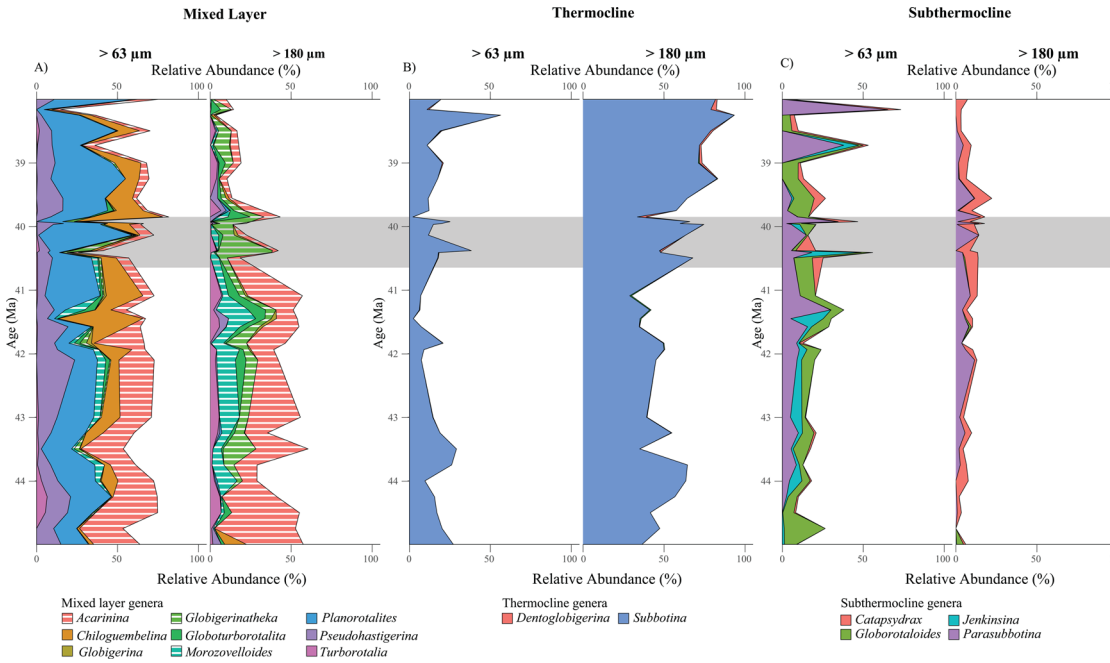

FIGURE 4. Relative abundance plots of genera across the North Atlantic middle Eocene from International Ocean Discovery Program (IODP) Expedition 342 Sites U1406, U1408, and U1410 separated by depth habitat and size fraction. A, Surface dwellers with symbiont-bearing taxa filled with a pattern; B, thermocline dwellers; C, subthermocline dwellers. Note different color schemes are used per depth habitat for ease of viewing. Symbiont-bearing foraminifera: *Acarinina*, *Morozovelloides*, and *Globigerinatheka* are indicated by a striped pattern. The gray horizontal box represents the middle Eocene climatic optimum (MECO) interval. *Turborotalita*, *Orbulinoides*, and *Hantkenina* are not included in this plot, as they occurred in such low numbers (1–5 absolute abundance).

Tables 2–8). In addition, we found that analytical choice of size fraction resulted in apparent differences in planktonic foraminifera response to both MECO warming and post-MECO cooling (Figs. 2, 3). The loss of symbiont-bearing foraminifera only changes depth-habitat diversity in the >180 µm size fraction (Fig. 3F), because these genera are replaced in the mixed layer by increased numbers of nonsymbiotic *Chiloguembelina* and *Planorotalites* in the >63 µm size fraction (Fig. 4).

Influence of Dissolution on Diversity Analysis

Dissolution has the potential to shift planktonic foraminiferal assemblages from representing environmentally shaped life assemblages to taphonomically shaped death assemblages (Berger 1971; Thunell 1976), biasing climatic and biotic interpretations of these assemblages (Berger 1973). Dissolution can be morphologically selective (Berger 1970; Boltovskoy and Totah 1992; Petrizzo et al. 2008; Nguyen et al. 2009, 2011, but see Petro et al. 2018) with species-specific tendencies (Nguyen et al. 2011; but see Berger 1970; Malmgren 1987). Across the MECO, extensive dissolution as a result of shoaling CCD has been recorded in the Pacific, Indian, and Atlantic Oceans (Lyle et al. 2005; Bohaty et al. 2009; Pälike et al. 2012). Despite our study sites sitting well above the known late Paleogene CCD (Norris et al. 2014), we still find that ~11% of our samples (7 out of 66) had higher fragmentation than what is considered normal for a well-preserved sample (Pfuhl and Shackleton 2004). While this indicates some degree of dissolution, probably reflecting increased carbonate dissolution due to the shoaling of the lysocline during the MECO (Boscolo Galazzo et al. 2013; Savian et al. 2014), there was no observable drop in overall planktonic foraminifera abundances, which would indicate dissolution impacted assemblages (Malmgren 1987). We do detect a statistically significant effect of dissolution in

https://doi.org/10.1017/pab.2022.24 Published online by Cambridge University Press

our statistical models, and recommend accounting for it in statistical analyses, but the small effect sizes (e.g., up to 55 times smaller than the effect of size fraction choice) and unchanged predictions when fragmentation is doubled and halved (Supplementary Figs. 13, 14) suggest that dissolution is not a strong driver of the diversity dynamics we report (Figs. 2–4).

Transient Climate Impacts on Specialist Feeding Ecologies

Our samples are the first midlatitude open-ocean samples analyzed for assemblages across the middle Eocene. Therefore, our results give a unique insight into the impacts of the MECO on symbiont-bearing foraminifera (*Acarinina*, *Morozovelloides*, and *Globigerinatheka*) and motivation for further studies at high-latitude sites.

We observe abundance decreases on the Newfoundland margin before the MECO at ~40.50 Ma in the >180 µm size fraction and at ~41.31 Ma in the >63 µm size fraction that persist post-MECO (Fig. 4, Supplementary Tables 3, 4). At the lower latitude Ocean Drilling Program Site 1051 in the North Atlantic Ocean (~25°N, Blake Nose), large *Acarinina* (>300 µm) abundance only temporarily decreases during peak warming of the MECO (Edgar et al. 2013); in the subtropical Alano section, the abundance of *Acarinina* is high before and during the MECO, but then abruptly decreases post-MECO and remains low (Luciani et al. 2010). Our observed decline in abundance is notably smaller on the Newfoundland margin in the North Atlantic (~20% reduction in *Acarinina*) compared with the subtropical Alano section. *Acarinina* relative abundance never recovers following the decline in our record, instead staying consistently low as in the Tethys (Luciani et al. 2010; Fig. 4), unlike the lower-latitude Blake Nose (~25°N), where *Acarinina* recovers in both abundance and test size (Edgar et al. 2013). Though not as abundant as *Acarinina*, *Morozovelloides* is present in our samples, with a peak relative abundance in both size fractions at 41.31 Ma before the MECO (~20% in the >180 µm fraction and ~11% in the >63 µm fraction; Fig. 4), followed by a decline in relative abundance through MECO warming, despite being thermophilic, and to the end of our record (Fig. 4). The general trend of post-MECO reduction in relative abundance of *Morozovelloides* is observed at other localities (Wade et al. 2008; Luciani et al. 2010; Edgar et al. 2013), although in the Tethys, *Morozovelloides* is scarcely abundant throughout the middle Eocene (Luciani et al. 2010; Gebhardt et al. 2013). The low relative abundances observed in *Morozovelloides* here and at Tethys sites (Luciani et al. 2010; Gebhardt et al. 2013) are therefore likely a result of these subtropical sites being at the ecological limit for the thermophilic *Morozovelloides*. The biogeographic differences in population dynamics between these two seemingly ecologically similar genera emphasizes the need for spatially replicated ecological sampling.

Stable isotope data, though limited, show that *Acarinina* and *Morozovelloides* at Site U1408 had the expected size–$\delta^{13}C$ relationship of dinoflagellate symbiont bearers during the MECO (Henehan et al. 2020). Mixotrophy, or the harboring of photosymbiotic algae, is relatively common in modern planktonic foraminifera (Takagi et al. 2019) and has been a key component for shaping spatial and temporal diversity patterns (Ezard et al. 2011; Fenton et al. 2016b; Hannisdal et al. 2017). Despite its continual occurrence throughout geological time in this study, we classify mixotrophy as a specialist, adaptive ecological feeding strategy, as it limits the planktonic foraminifera to a narrow ecological niche (Raia et al. 2016; Rolland and Salamin 2016). During the middle Eocene, mixotrophic foraminifera likely included *Acarinina*, *Morozovelloides*, *Globigerinatheka*, and *Orbulinoides*, all of which experienced major global changes in their relative abundance and ecology as a result of transient climate change (Keller 1983; Boersma and Silva 1991; Wade 2004; Wade and Pearson 2008; Wade and Olsson 2009; Luciani et al. 2010; Boscolo Galazzo et al. 2013; Edgar et al. 2013), with all (barring several small *Acarinina* species) becoming extinct before the end of the Eocene (Wade 2004; Wade and Pearson 2008).

Based on the shared ecological strategy of *Acarinina* and *Morozovelloides*, one conclusion may be that the reduction of these species at our site was a result of their specialist ecology and changes to their symbiotic relationship

https://doi.org/10.1017/pab.2022.24 Published online by Cambridge University Press

(Wade 2004; Wade et al. 2008; Edgar et al. 2013), as shown by reduction in test size–$\delta^{13}C$ relationship following the MECO at Blake Nose, Site 1051, in the northwest Atlantic (Edgar et al. 2013), that occurred as non–symbiont bearing surface layer dwellers continued to thrive (Fig. 4). Yet, despite sharing a similar specialist mixotrophic ecology, *Globigerinatheka* shows a peak in relative abundance of 33%–34% in the >180 μm size fraction and 11% in the >63 μm size fraction at ~40.40 Ma coincident with peak MECO warming (Fig. 4). In addition, other global records reflect dominance or relative abundance increases of *Globigerinatheka* through the MECO (Boersma and Premoli Silva 1986; Boersma et al. 1987; Edgar et al. 2013; Galazzo et al. 2014).

Specialist feeding ecologies have been cited as the reason for extinction in deep time of herbivorous sea urchins (Smith and Jeffery 1998), herbivorous insects (Labandeira et al. 2002), hypercarnivorous canids (Van Valkenburgh 2004), and crinoids (Baumiller 1993). A similar pattern of feeding specialist extinction has also been documented in planktonic foraminifera (Norris 1992), but Norris defined a specialist as foraminifera that has limited food sources. The success of *Globigerinatheka* and persistence of *Acarinina* and *Morozovelloides* suggests that specialization is not always entirely detrimental for organisms during transient climatic changes, even with large fluctuations in climate state. The decline in symbiont-bearing planktonic foraminifera across the middle Eocene does suggest the climatic fluctuations pushed these genera closer to their ecological limits (Ezard et al. 2011; Edgar et al. 2013), which was a process exaggerated at our sites due to the relatively high latitude locality near the species' biogeographic range limits.

Divergent Response of Size Fraction to the Middle Eocene

Assemblage studies are often conducted at size fractions above >150 μm to avoid juvenile specimens (Al-Sabouni et al. 2007), yet this coarse filter can remove large amounts of diversity and bias studies toward larger individuals, particularly at higher latitudes, where taxa are known to be smaller (Schmidt et al. 2004). In addition, sampling at a biotically uninformative size fraction can impact inferences on how communities respond to background, transient, and rapid environmental fluctuations. In this study, we found different timings of assemblage responses to middle Eocene climate as a result of size fraction (Figs. 2, 3).

At the relatively high latitude position of our site, water-column heterogeneity was already low due to the general lack of a substantial thermocline at higher latitudes (Rutherford et al. 1999; Al-Sabouni et al. 2007). Background Eocene cooling (Westerhold et al. 2020) would have increased water-column stratification, allowing for an increase in relative abundance of genera as a result of widening ecological niches (Whittaker et al. 2001; Al-Sabouni et al. 2007). We see the effects of increasing thermal stratification in the larger size fraction (>180 μm), where generic and morphological H_S and H_{GS} increase at 42.20 Ma (Fig. 2B,C,E, F). Long-term cooling of the Eocene coupled with thermal stratification and cooling increase before the MECO (Arimoto et al. 2020; Kearns et al. 2021) results in the removal of larger symbiont-bearing foraminifera (*Acarinina* and *Morozovelloides*) and a decline in generic and morphological H_S and H_{GS} (Fig. 3). These results imply that amplitude and intensity of environmental change has a major role on how ecosystems respond, possibly larger than the direction of change (Gibbs et al. 2012; Garcia et al. 2014; Mayfield et al. 2021).

In contrast, we do not see any consistent changes in effective diversity at multiple levels of q (Fig. 3) and no substantive differences between pre-MECO and MECO intervals (Fig. 3, Supplementary Table 25). Instead, effective diversity shows significant change in the post-MECO interval (Fig. 3, Supplementary Table 25) with a decrease in morphological, generic, and depth-habitat effective diversity at all levels ($q = 0$–2) and decreasing assemblage evenness. This trend to less-even communities follows the removal of large symbiont-bearing forms (Fig. 4) and an increase in thermocline dwellers at the expense of mixed-layer species (Fig. 4)

We observe no impact of general Eocene cooling or enhanced pre-MECO cooling on traditional diversity measures in the smaller size fraction compared with the >180 μm size

https://doi.org/10.1017/pab.2022.24 Published online by Cambridge University Press

fraction (Fig. 2). In addition, we see no impact of pre-MECO cooling on effective diversity (Fig. 3, Supplementary Table 25). Instead, we observe peaks on morphological and generic richness coinciding with peak MECO warming (Fig. 2A,D). Though the magnitude of warming experienced during the MECO at the sites drilled on IODP Expedition 342 is debated (Arimoto et al. 2020; Kearns et al. 2021), a global surface ocean temperature increase, alongside the removal of key large symbiont-bearing planktonic foraminifera, may have increased the number of vacant ecological niches, leading to increases in rare, small, microperforate surface-dwelling taxa alongside increases in thermocline dwellers. As a result of the transient nature of the MECO, which lasted ~270–500 kyr (Bohaty and Zachos 2003; Bohaty et al. 2009; Westerhold and Röhl 2013; Rivero-Cuesta et al. 2019; Edgar et al. 2020), test size increases in response to increasing warmth, and thus emergence of potentially ecologically optimum conditions, are not observed, unlike at other periods in geological history (Schmidt et al. 2003; Al-Sabouni et al. 2007; Todd et al. 2020). A lack of size response as a result of decreasing thermal stratification across the MECO at this site (Arimoto et al. 2020; Kearns et al. 2021) was a driver of globally small test sizes in the middle Eocene (Schmidt et al. 2004) and was responsible for the emergence of a latitudinal size gradient at ~42 Ma that persists today (Schmidt et al. 2004). The brevity of the MECO also meant increasing diversity in the >63 µm size fraction was short-lived and was followed by a dramatic decline in generic and morphological richness (Fig. 3A,D) and effective diversity (q <1; Fig. 3). Post-MECO cooling had little other effect on effective diversity, except a reduction in morphological diversity ($q = 1$–2) as a result of the decline in morphologically distinct *Chiloguembelina* and *Jenkinsina*.

Insights into Paleoceanographic Changes across the MECO from "Rare" Taxa

In our record, we have numerous genera with low occurrence (~8 genera) that could be considered rare and cause large fluctuations in generic and morphogroup effective diversity ($q = 0$) at both size fractions (Figs. 2, 3). Although rarity in itself is potentially an important measure (e.g., acting as canaries for early warning signals; Doncaster et al. 2016), being rare is common, with the majority of taxa represented by only a few individuals (Gaston 2008). Microperforate biserial and triserial taxa such as *Chiloguembelina* and *Jenkinsina* are rare in many records, as they occur in highest abundance in the infrequently studied >63 µm size fraction despite being omnipresent throughout the Cenozoic (Li and Radford 1991), with approximately 20 species occurring in the Eocene alone (Huber et al. 2006). In addition, these taxa have sporadic geographic and biostratigraphic records (Kroon and Nederbragt 1990; Darling et al. 2009), often increasing to noticeable abundances during periods of environmental stress such as ocean acidification events (Nederbragt et al. 1998; Coccioni et al. 2006), periods of background climatic instability (Kroon and Nederbragt 1990; Li and Radford 1991; Luciani et al. 2007, 2010; D'Haenens et al. 2012), and the aftermath of mass extinction events (Keller 1993; Luciani 1997, 2002; Keller et al. 2002). The lack of changes at the >63 µm size fraction for most diversity measures compared with the >180 µm size fraction supports these results that smaller taxa are more resilient to both background (i.e., Eocene cooling) and transient perturbations (MECO) compared with large taxa and thus deserving of further study.

In our record, both *Chiloguembelina* and *Jenkinsina* are only substantive components of assemblages in the >63 µm size fraction (Fig. 4), not at >180 µm. Two noticeable peaks occur in *Chiloguembelina* (43.24% at 39.85 Ma and 52.27% at 41.45 Ma) and *Jenkinsina* (30.42% at 40.41 Ma and 20.05% at 41.45 Ma), coinciding with paleoceanographic instability across the MECO, interrupting otherwise relatively low relative abundances (*Chiloguembelina*: <~20%, *Jenkinsina*: <~1%; Fig. 4). Similar peaks in abundance of *Chiloguembelina* and *Jenkinsina* have been observed in the Tethys Ocean (Alano section; Luciani et al. 2010) and at other high-latitude sites (Li and Radford 1991) and associated with upwelling or low-oxygen conditions. There is no evidence for either at our study site (Arimoto et al. 2020; Kearns et al. 2021), but these peaks in abundance support

https://doi.org/10.1017/pab.2022.24 Published online by Cambridge University Press

arguments that these taxa thrive during transient climatic events.

One hypothesis as to why rare taxa flourish during environmental perturbations is that they replace superior predators or dominant taxa that are lost in order to maintain ecological function (Walker et al. 1999). Both *Chiloguembelina* relative abundance peaks occur synchronously with troughs in *Acarinina* relative abundance (Fig. 4). As all three genera (*Chiloguembelina*, *Morozovelloides*, and *Acarinina*) are surface dwelling, this rise in abundance may be a response to the sparsely occupied ecological niche(s) left by the removal of a large proportion of *Acarinina* and *Morozovelloides*. This synchronicity may reflect changes in surface-water productivity, as *Chiloguembelina* is an opportunistic eutrophic genus (Luciani et al. 2020). Coincidental changes in relative abundance also occur in the thermocline and subthermocline, where *Jenkinsina* peaks at the same time as *Subbotina* (Fig. 4). While no taxa are removed from the thermocline during the MECO, *Subbotina* has a wide and plastic ecological niche (Kearns et al. 2021), and it may be that *Jenkinsina* prospered for a short interval due to temporary availability of the thermocline ecological niche. Stable isotope studies of *Chiloguembelina* and *Jenkinsina* across the middle Eocene would be one route to rigorously testing this hypothesis. Our observations do suggest, however, that these rara taxa are useful when looking at paleoceanographic changes to identify periods of environmental instability and therefore should be measured instead of being dismissed for their small size and sporadic geographic and biostratigraphic records (Kroon and Nederbragt 1990; Darling et al. 2009).

Conclusion

Our analysis of planktonic foraminiferal assemblages within the middle Eocene at sites on the Newfoundland margin demonstrate that complex diversity dynamics follow transient environmental changes. We show that transient events are not necessarily terminal for specialist taxa but can push these taxa to their ecological limits, which potentially influences their abundance and community composition for millions of years after a transient perturbation. We argue that rather than complicating our understanding of planktonic foraminifera responses in the middle Eocene, measuring at two size fractions illuminates size dynamics more fully to enhance our understanding of paleooceanographic drivers of biotic turnover. The impact of rare taxa is not well described by its standing percentage in a community. However, by documenting the smaller size fraction, we were able to record smaller and more microperforate taxa, not normally measured, to show how rare taxa can provide equivalent ecological function to those taxa that are lost and inform our understanding of environmental perturbations and how communities to persist through climate fluctuations.

Acknowledgments

This research used samples provided by the IODP. We would like to thank A. Brombacher and M. Holmström for taxonomic guidance. We would also like to thank M. Yasuhara and one anonymous reviewer for their helpful comments when reviewing this article. This work was supported by the Natural Environment Research Council awards NE/L002531/1 and NE/P019269/1, as well as the Institute of Life Sciences (IfLS) at the University of Southampton. The authors declare no competing interests.

Data Availability Statement

Data available from the Dryad digital repository: https://doi.org/10.5061/dryad.cfxpnvx81.

Literature Cited

Al-Sabouni, N., M. Kucera, and D. N. Schmidt. 2007. Vertical niche separation control of diversity and size disparity in planktonic foraminifera. Marine Micropaleontology 63:75–90.

Al-Sabouni, N., I. S. Fenton, R. J. Telford, and M. Kučera. 2018. Reproducibility of species recognition in modern planktonic foraminifera and its implications for analyses of community structure. Journal of Micropalaeontology 37:519–534.

Arimoto, J., H. Nishi, A. Kuroyanagi, R. Takashima, H. Matsui, and M. Ikehara. 2020. Changes in upper ocean hydrography and productivity across the Middle Eocene Climatic Optimum: local insights and global implications from the northwest Atlantic. Global and Planetary Change 193:1–12.

Aze, T., T. H. G. Ezard, A. Purvis, H. K. Coxall, D. R. M. Stewart, B. S. Wade, and P. N. Pearson. 2011. A phylogeny of Cenozoic macroperforate planktonic foraminifera from fossil data. Biological Reviews 86:900–927.

Baum, D. A. 2009. Species as ranked taxa. Systematic Biology 58:74–86.

https://doi.org/10.1017/pab.2022.24 Published online by Cambridge University Press

Baumiller, T. K. 1993. Survivorship analysis of Paleozoic Crinoidea: effect of filter morphology on evolutionary rates. Paleobiology 19:304–321.

Berger, W. H. 1970. Planktonic foraminifera: Selective solution and the lysocline. Marine Geology 8:111–138.

Berger, W. H. 1971. Sedimentation of planktonic foraminifera. Marine Geology 11:325–358.

Berger, W. H. 1973. Deep-sea carbonates: Pleistocene dissolution cycles. Journal of Foraminiferal Research 3:187–195.

Bijl, P. K., A. J. P. Houben, S. Schouten, S. M. Bohaty, A. Sluijs, G.-J. Reichart, J. S. S. Damsté, and H. Brinkhuis. 2010. Transient middle Eocene atmospheric CO_2 and temperature variations. Science 330:819–821.

Boersma, A., and I. P. Silva. 1986. Terminal Eocene events: planktonic foraminifera and isotopic evidence. Developments in Palaeontology and Stratigraphy 9:213–223.

Boersma, A., and I. P. Silva. 1991. Distribution of Paleogene planktonic foraminifera— analogies with the Recent? Palaeogeography, Palaeoclimatology, Palaeoecology 83:29–48.

Boersma, A., I. P. Silva, and N. J. Shackleton. 1987. Atlantic Eocene planktonic foraminiferal paleohydrographic indicators and stable isotope paleoceanography. Paleoceanography 2:287–331.

Bohaty, S. M., and J. C. Zachos. 2003. Significant Southern Ocean warming event in the late middle Eocene. Geology 31:1017–1020.

Bohaty, S. M., J. C. Zachos, F. Florindo, and M. L. Delaney. 2009. Coupled greenhouse warming and deep-sea acidification in the middle Eocene. Paleoceanography 24:1–16.

Boltovskoy, E., and V. I. Totah. 1992. Preservation index and preservation potential of some foraminiferal species. Journal of Foraminiferal Research 22:267–273.

Boscolo Galazzo, F., L. Giusberti, V. Luciani, and E. Thomas. 2013. Paleoenvironmental changes during the Middle Eocene Climatic Optimum (MECO) and its aftermath: the benthic foraminiferal record from the Alano section (NE Italy). Palaeogeography, Palaeoclimatology, Palaeoecology 378:22–35.

Boyle, P. R., B. W. Romans, B. E. Tucholke, R. D. Norris, S. A. Swift, and P. F. Sexton. 2017. Cenozoic North Atlantic deep circulation history recorded in contourite drifts, offshore Newfoundland, Canada. Marine Geology 385:185–203.

Brummer, G. A., C. Hemlebent, and M. Spindlert. 1986. Planktonic foraminiferal ontogeny and new perspectives for micropalaeontology. Nature 319:50–52.

Brummer, G.-J. A., and M. Kučera. 2022. Taxonomic review of living planktonic foraminifera. Journal of Micropalaeontology 41:29–74.

Burnham, K., and D. Anderson. 2002. Model selection and multimodel inference. Springer, New York.

Chao, A., and L. Jost. 2012. Diversity measures. Pp. 203–207 *in* Encyclopedia of theoretical ecology. University of California Press, Berkeley.

Chao, A., and L. Jost. 2015. Estimating diversity and entropy profiles via discovery rates of new species. Methods in Ecology and Evolution 6:873–882.

Chao, A., C. H. Chiu, and L. Jost. 2010. Phylogenetic diversity measures based on Hill numbers. Philosophical Transactions of the Royal Society of London B 365:3599–3609.

Chao, A., C.-H. Chiu, and L. Jost. 2014a. Unifying species diversity, phylogenetic diversity, functional diversity, and related similarity and differentiation measures through Hill numbers. Annual Review of Ecology, Evolution and Systematics 45:297–324.

Chao, A., N. J. Gotelli, T. C. Hsieh, E. L. Sander, R. K. Colwell, and A. M. Ellison. 2014b. Rarefaction and extrapolation with Hill numbers: a framework for sampling and estimation in species diversity studies. Ecological Monographs 84:45–67.

Chao, A., Y. Kubota, D. Zelený, C.-H. Chiu, C.-F. Li, B. Kusumoto, M. Yasuhara, S. Thorn, C.-L. Wei, M. J. Costello, and R. K. Colwell. 2020. Quantifying sample completeness and comparing diversities among assemblages. Ecological Research 35:292–314.

Chiarucci, A., G. Bacaro, and S. M. Scheiner. 2011. Old and new challenges in using species diversity for assessing biodiversity. Philosophical Transactions of the Royal Society of London B 366:2426–2437.

Chiu, C. H., and A. Chao. 2014. Distance-based functional diversity measures and their decomposition: a framework based on Hill numbers. PLoS ONE 9:1–17.

Coccioni, R., V. Luciani, and A. Marsili. 2006. Cretaceous oceanic anoxic events and radially elongated chambered planktonic foraminifera: paleoecological and paleoceanographic implications. Palaeogeography, Palaeoclimatology, Palaeoecology 235:66–92.

Colwell, R. K. 2009. Biodiversity: concepts, patterns, and measurement. Pp. 257–263 *in* The Princeton guide to ecology. Princeton University Press, Princeton, N.J.

Colwell, R. K., J. A. Coddington, and D. L. Hawksworth. 1994. Estimating terrestrial biodiversity through extrapolation. Philosophical Transactions of the Royal Society of London B 345:101–118.

Coxall, H. K., P. N. Pearson, N. J. Shackleton, and M. A. Hall. 2000. Hantkeninid depth adaptation: an evolving life strategy in a changing ocean. Geology 28:87–90.

Coxall, H. K., P. A. Wilson, H. Pälike, C. H. Lear, J. Backman, and A. Arrhenius. 2005. Rapid stepwise onset of Antarctic glaciation and deeper calcite compensation in the Pacific Ocean. Nature 433:53–57.

Cramwinckel, M. J., R. van der Ploeg, P. K. Bijl, F. Peterse, S. M. Bohaty, U. Röhl, S. Schouten, J. J. Middelburg, and A. Sluijs. 2019. Harmful algae and export production collapse in the equatorial Atlantic during the zenith of Middle Eocene Climatic Optimum warmth. Geology 47:247–250.

Darling, K. F., E. Thomas, S. A. Kasemann, H. A. Seears, C. W. Smart, and C. M. Wade. 2009. Surviving mass extinction by bridging the benthic/planktic divide. Proceedings of the National Academy of Sciences USA 106:12629–12633.

D'Haenens, S., A. Bornemann, K. Roose, P. Claeys, and R. P. Speijer. 2012. Stable isotope paleoecology ($\delta^{13}C$ and $\delta^{18}O$) of early Eocene *Zeauvigerina aegyptiaca* from the north Atlantic (DSDP site 401). Austrian Journal of Earth Sciences 105:179–188.

Doncaster, C. P., V. A. Chávez, C. Viguier, R. Wang, E. Zhang, X. Dong, J. A. Dearing, P. G. Langdon, and J. G. Dyke. 2016. Early warning of critical transitions in biodiversity from compositional disorder. Ecology 97:3079–3090.

Edgar, K. M., S. M. Bohaty, S. J. Gibbs, P. F. Sexton, R. D. Norris, and P. A. Wilson. 2013. Symbiont "bleaching" in planktic foraminifera during the Middle Eocene Climatic Optimum. Geology 41:15–18.

Edgar, K. M., S. M. Bohaty, H. K. Coxall, P. R. Bown, S. J. Batenburg, C. H. Lear, and P. N. Pearson. 2020. New composite bio- and isotope stratigraphies spanning the Middle Eocene Climatic Optimum at tropical ODP Site 865 in the Pacific Ocean. Journal of Micropalaeontology 39:117–138.

Ellison, A. M. 2010. Partitioning diversity. Ecology 91:1962–1963.

Ezard, T. H. G., T. Aze, P. N. Pearson, and A. Purvis. 2011. Interplay between changing climate and species' ecology drives macroevolutionary dynamics. Science 332:349–351.

Fenton, I. S., P. N. Pearson, T. Dunkley Jones, A. Farnsworth, D. J. Lunt, P. Markwick, and A. Purvis. 2016a. The impact of Cenozoic cooling on assemblage diversity in planktonic foraminifera. Philosophical Transactions of the Royal Society of London B 371:20150224.

Fenton, I. S., P. N. Pearson, T. Dunkley Jones, and A. Purvis. 2016b. Environmental predictors of diversity in recent planktonic foraminifera as recorded in marine sediments. PLoS ONE 11:1–22.

Fenton, I. S., A. Woodhouse, T. Aze, D. Lazarus, J. Renaudie, A. M. Dunhill, J. R. Young, and E. E. Saupe. 2021. Triton, a new

https://doi.org/10.1017/pab.2022.24 Published online by Cambridge University Press

species-level database of Cenozoic planktonic foraminiferal occurrences. Scientific Data 8:160.

Fraass, A. J., D. C. Kelly, and S. E. Peters. 2015. Macroevolutionary history of the planktic Foraminifera. Annual Review of Earth and Planetary Sciences 43:139–166.

Galazzo, F. B., E. Thomas, M. Pagani, C. Warren, V. Luciani, and L. Giusberti. 2014. The middle Eocene climatic optimum (MECO): a multiproxy record of paleoceanographic changes in the southeast Atlantic (ODP Site 1263, Walvis Ridge). Paleoceanography and Paleoclimatology 29:1143–1161.

Galazzo, F. B., E. Thomas, V. Luciani, L. Giusberti, F. Frontalini, and R. Coccioni. 2015. The planktic foraminifer *Planorotalites* in the Tethyan middle Eocene. Journal of Micropalaeontology 35:79–89.

Garcia, R. A., M. Cabeza, C. Rahbek, and M. B. Araújo. 2014. Multiple dimensions of climate change and their implications for biodiversity. Science 344:1247579.

Gaston, K. J. 2008. Biodiversity and extinction: the importance of being common. Progress in Physical Geography 32:73–79.

Gaston, K. J., and R. A. Fuller. 2007. Biodiversity and extinction. Progress in Physical Geography 31:213–225.

Gebhardt, H., S. Ćorić, R. Darga, A. Briguglio, B. Schenk, W. Werner, N. Andersen, and B. Sames. 2013. Middle to Late Eocene paleoenvironmental changes in a marine transgressive sequence from the northern Tethyan margin (Adelholzen, Germany). Austrian Journal of Earth Sciences 106:45–72.

Gibbs, S. J., P. R. Bown, B. H. Murphy, A. Sluijs, K. M. Edgar, H. Pälike, C. T. Bolton, and J. C. Zachos. 2012. Scaled biotic disruption during early Eocene global warming events. Biogeosciences 9:4679–4688.

Gradstein, F. M., J. G. Ogg, M. D. Schmitz, and G. M. Ogg. 2012. The geologic time scale 2012. Elsevier, Amsterdam.

Hallock, P., I. P. Silva, and A. Boersma. 1991. Similarities between planktonic and larger foraminiferal evolutionary trends through Paleogene paleoceanographic changes. Palaeogeography, Palaeoclimatology, Palaeoecology 83:49–64.

Hannisdal, B., K. A. Haaga, T. Reitan, D. Diego, and L. H. Liow. 2017. Common species link global ecosystems to climate change: dynamical evidence in the planktonic fossil record. Proceedings of the Royal Society of London B 284:20170722.

Hendricks, J. R., E. E. Saupe, C. E. Myers, E. J. Hermsen, and W. D. Allmon. 2014. The generification of the fossil record. Paleobiology 40:511–528.

Henehan, M. J., K. M. Edgar, G. L. Foster, D. E. Penman, P. M. Hull, R. Greenop, E. Anagnostou, and P. N. Pearson. 2020. Revisiting the Middle Eocene Climatic Optimum "carbon cycle conundrum" with new estimates of atmospheric pCO_2 from boron isotopes. Paleoceanography and Paleoclimatology 35:1–22.

Heritier-Robbins, P., S. Karthikeyan, J. K. Hatt, M. Kim, M. Huettel, J. E. Kostka, K. T. Konstantinidis, and L. M. Rodriguez-R. 2021. Beach sand oil spills select for generalist microbial populations. ISME Journal 15:3418–3422.

Hill, M. O. 1973. Diversity and evenness: a unifying notation and its consequences. Ecology 54:427–432.

Hohenegger, J. 2014. Species as the basic units in evolution and biodiversity: recognition of species in the Recent and geological past as exemplified by larger foraminifera. Gondwana Research 25:707–728.

Hong, Y., M. Yasuhara, H. Iwatani, A. Chao, P. G. Harnik, and C.-L. Wei. 2021. Ecosystem turnover in an urbanized subtropical seascape driven by climate and pollution. Anthropocene 36:100304.

Huber, B. T., R. K. Olsson, and P. N. Pearson. 2006. *Taxonomy, biostratigraphy, and phylogeny of Eocene microperforate planktonic foraminifera* (Jenkinsina, Cassigerinelloita, Chiloguembelina, Streptochilus, Zeauvigerina, Tenuitella *and* Cassigerinella*) and problematic* (Dipsidripella). Pp. 461–508 *in* P. N. Pearson, R. K. Olsson, B. T. Huber, C. Hemleben, and W. A. Berggren. Atlas of Eocene planktonic foraminifera. Cushman Foundation for Foraminiferal Research, Vol. 41. GeoScience World, McLean, Va.

Hutchinson, D. K., H. K. Coxall, D. J. Lunt, M. Steinthorsdottir, A. M. de Boer, M. Baatsen, A. von der Heydt, M. Huber, A. T. Kennedy-Asser, L. Kunzmann, J.-B. Ladant, C. H. Lear, K. Moraweck, P. N. Pearson, E. Piga, M. J. Pound, U. Salzmann, H. D. Scher, W. P. Sijp, K. K. Śliwińska, P. A. Wilson, and Z. Zhang. 2021. The Eocene–Oligocene transition: a review of marine and terrestrial proxy data, models and model–data comparisons. Climate of the Past 17:269–315.

Ishino, S., and I. Suto. 2020. Late Pliocene sea-ice expansion and its influence on diatom species turnover in the Southern Ocean. Marine Micropaleontology 160:101895.

Jackson, S. T., and J. L. Blois. 2015. Community ecology in a changing environment: perspectives from the Quaternary. Proceedings of the National Academy of Sciences USA 112:4915–4921.

Jost, L. 2007. Partitioning diversity into independent alpha and beta components. Ecology 88:2427–2439.

Jost, L. 2010a. Independence of alpha and beta diversities. Ecology 91:1969–1974.

Jost, L. 2010b. The relation between evenness and diversity. Diversity 2:207–232.

Kang, S., J. L. M. Rodrigues, J. P. Ng, and T. J. Gentry. 2016. Hill number as a bacterial diversity measure framework with high-throughput sequence data. Scientific Reports 6:38263.

Kearns, L. E., S. M. Bohaty, K. M. Edgar, S. Nogué, and T. H. G. Ezard. 2021. Searching for function: reconstructing adaptive niche changes using geochemical and morphological data in planktonic foraminifera. Frontiers in Ecology and Evolution 9:1–17.

Keller, G. 1983. Paleoclimatic analyses of middle Eocene through Oligocene planktic foraminiferal faunas. Palaeogeography, Palaeoclimatology, Palaeoecology 43:73–94.

Keller, G. 1993. The Cretaceous–Tertiary boundary transition in the Antarctic Ocean and its global implications. Marine Micropaleontology 21:1–45.

Keller, G., N. MacLeod, and E. Barrera. 1992. Eocene–Oligocene faunal turnover in planktic Foraminifera, and Antarctic glaciation. Pp. 218–244 *in* D. R. Prothero and W. A. Berggren, eds. Eocene–Oligocene climatic and biotic evolution. Princeton University Press, Princeton, N.J.

Keller, G., T. Adatte, W. Stinnesbeck, V. Luciani, N. Karoui-Yaakoub, and D. Zaghbib-Turki. 2002. Paleoecology of the Cretaceous–Tertiary mass extinction in planktonic foraminifera. Palaeogeography, Palaeoclimatology, Palaeoecology 178:257–297.

Kroon, D., and A. J. Nederbragt. 1990. Ecology and paleoecology of triserial planktic foraminifera. Marine Micropaleontology 16:25–38.

Kucera, M. 2007. Planktonic foraminifera as tracers of past oceanic environments. Pp. 213–262 *in* C. Hillaire–Marcel and A. De Vernal, eds. Proxies in Late Cenozoic paleoceanography. Developments in Marine Geology, Vol. 1. Elsevier, Amsterdam.

Kucera, M., M. Weinelt, T. Kiefer, U. Pflaumann, A. Hayes, M. Weinelt, M.-T. Chen, A. C. Mix, T. T. Barrows, E. Cortijo, J. Duprat, S. Juggins, and C. Waelbroeck. 2005. Reconstruction of sea-surface temperatures from assemblages of planktonic foraminifera: multi-technique approach based on geographically constrained calibration data sets and its application to glacial Atlantic and Pacific Oceans. Quaternary Science Reviews 24:951–998.

Labandeira, C. C., K. R. Johnson, and P. Wilf. 2002. Impact of the terminal Cretaceous event on plant-insect associations. Proceedings of the National Academy of Sciences USA 99:2061–2066.

Le, J., and N. J. Shackleton. 1992. Carbonate dissolution fluctuations in the western equatorial Pacific during the Late Quaternary. Paleoceanography 7:21–42.

https://doi.org/10.1017/pab.2022.24 Published online by Cambridge University Press

Lennon, J. J., P. Koleff, J. J. D. Greenwood, and K. J. Gaston. 2004. Contribution of rarity and commonness to patterns of species richness. Ecology Letters 7:81–87.

Leon-Rodriguez, L., and G. R. Dickens. 2010. Constraints on ocean acidification associated with rapid and massive carbon injections: the early Paleogene record at Ocean Drilling Program Site 1215, equatorial Pacific Ocean. Palaeogeography, Palaeoclimatology, Palaeoecology 298:409–420.

Li, Q. Y., and S. S. Radford. 1991. Evolution and biogeography of Paleogene microperforate planktonic-foraminifera. Palaeogeography, Palaeoclimatology, Palaeoecology 83:87–115.

Luciani, V. 1997. Planktonic foraminiferal turnover across the Cretaceous–Tertiary boundary in the Vajont valley (southern Alps, northern Italy). Cretaceous Research 18:799–821.

Luciani, V. 2002. High-resolution planktonic foraminiferal analysis from the Cretaceous–Tertiary boundary at Ain Settara (Tunisia): evidence of an extended mass extinction. Palaeogeography, Palaeoclimatology, Palaeoecology 178:299–319.

Luciani, V., L. Giusberti, C. Agnini, J. Backman, E. Fornaciari, and D. Rio. 2007. The Paleocene–Eocene Thermal Maximum as recorded by Tethyan planktonic foraminifera in the Forada section (northern Italy). Marine Micropaleontology 64:189–214.

Luciani, V., L. Giusberti, C. Agnini, E. Fornaciari, D. Rio, D. J. A. Spofforth, and H. Pälike. 2010. Ecological and evolutionary response of Tethyan planktonic foraminifera to the middle Eocene climatic optimum (MECO) from the Alano section (NE Italy). Palaeogeography, Palaeoclimatology, Palaeoecology 292:82–95.

Luciani, V., R. D'Onofrio, G. Filippi, and S. Moretti. 2020. Which was the habitat of early Eocene planktic foraminifer *Chiloguembelina*? Stable isotope paleobiology from the Atlantic Ocean and implication for paleoceanographic reconstructions. Global and Planetary Change 191:103216.

Lyle, M. W., A. Olivarez Lyle, J. Backman, and A. Tripati. 2005. Biogenic sedimentation in the Eocene equatorial Pacific: the stuttering greenhouse and Eocene carbonate compensation depth. Proceedings of the Ocean Drilling Program, Scientific Results 199:1–31.

Lyons, K. G., C. A. Brigham, B. H. Traut, and M. W. Schwartz. 2005. Rare species and ecosystem functioning. Conservation Biology 19:1019–1024.

Mace, G. M., K. Norris, and A. H. Fitter. 2012. Biodiversity and ecosystem services: a multilayered relationship. Trends in Ecology and Evolution 27:19–26.

Malmgren, B. A. 1987. Differential dissolution of upper Cretaceous planktonic foraminifera from a temperate region of the South Atlantic ocean. Marine Micropaleontology 11:251–271.

Mayfield, R. J., P. G. Langdon, C. P. Doncaster, J. A. Dearing, R. Wang, G. Velle, K. L. Davies, and S. J. Brooks. 2021. Late Quaternary chironomid community structure shaped by rate and magnitude of climate change. Journal of Quaternary Science 36:360–376.

Mayr, E. 1942. Systematics and the origin of species. Columbia University Press, New York.

McClain, C. R., C. Nunnally, and M. C. Benfield. 2019. Persistent and substantial impacts of the Deepwater Horizon oil spill on deep-sea megafauna. Royal Society Open Science 6:191164.

Miller, J. I., S. Techtmann, D. Joyner, N. Mahmoudi, J. Fortney, J. A. Fordyce, N. GaraJayeva, F. S. Askerov, C. Cravid, M. Kuijper, O. Pelz, and T. C. Hazen. 2020. Microbial communities across global marine basins show important compositional similarities by depth. MBio 11:1–12.

Nederbragt, A. J., R. N. Erlich, B. W. Fouke, and G. M. Ganssen. 1998. Palaeoecology of the biserial planktonic foraminifer *Heterohelix moremani* (Cushman) in the late Albian to middle Turonian Circum-North Atlantic. Palaeogeography, Palaeoclimatology, Palaeoecology 144:115–133.

Nguyen, T. M. P., and R. P. Speijer. 2014. A new procedure to assess dissolution based on experiments on Pliocene–Quaternary foraminifera (ODP Leg 160, Eratosthenes Seamount, eastern Mediterranean). Marine Micropaleontology 106:22–39.

Nguyen, T. M. P., M. R. Petrizzo, and R. P. Speijer. 2009. Experimental dissolution of a fossil foraminiferal assemblage (Paleocene–Eocene Thermal Maximum, Dababiya, Egypt): implications for paleoenvironmental reconstructions. Marine Micropaleontology 73:241–258.

Nguyen, T. M. P., M. R. Petrizzo, P. Stassen, and R. P. Speijer. 2011. Dissolution susceptibility of Paleocene–Eocene planktic foraminifera: implications for palaeoceanographic reconstructions. Marine Micropaleontology 81:1–21.

Norris, R. D. 1992. Extinction selectivity and ecology in planktonic foraminifera. Palaeogeography, Palaeoclimatology, Palaeoecology 95:1–17.

Norris, R. D., P. A. Wilson, P. Blum, and the Expedition 342 Scientists. 2014. Proceedings of the Integrated Ocean Drilling Program 342. Integrated Ocean Drilling Program, College Station, TX.

Ogle D. H., J. C. Doll, P. Wheeler, and A. Dinno. 2022. FSA: fisheries stock analysis, R package version 0.9.3. https://github.com/fishR-Core-Team/FSA.

Pälike, H., M. W. Lyle, H. Nishi, I. Raffi, A. Ridgwell, K. Gamage, A. Klaus, G. Acton, L. Anderson, J. Backman, J. Baldauf, C. Beltran, S. M. Bohaty, P. Bown, W. Busch, J. E. T. Channell, C. O. J. Chun, M. Delaney, P. Dewangan, T. Dunkley Jones, K. M. Edgar, H. Evans, P. Fitch, G. L. Foster, N. Gussone, H. Hasegawa, E. C. Hathorne, H. Hayashi, J. O. Herrle, A. Holbourn, S. Hovan, K. Hyeong, K. Iijima, T. Ito, S. I. Kamikuri, K. Kimoto, J. Kuroda, L. Leon-Rodriguez, A. Malinverno, T. C. Moore, B. H. Murphy, D. P. Murphy, H. Nakamura, K. Ogane, C. Ohneiser, C. Richter, R. Robinson, E. J. Rohling, O. Romero, K. Sawada, H. Scher, L. Schneider, A. Sluijs, H. Takata, J. Tian, A. Tsujimoto, B. S. Wade, T. Westerhold, R. Wilkens, T. Williams, P. A. Wilson, Y. Yamamoto, S. Yamamoto, T. Yamazaki, and R. E. Zeebe. 2012. A Cenozoic record of the equatorial Pacific carbonate compensation depth. Nature 488:609–614.

Pärtel, M., R. Szava-Kovats, and M. Zobel. 2011. Dark diversity: shedding light on absent species. Trends in Ecology and Evolution 26:124–128.

Patzkowsky, M. E., and S. M. Holland. 2007. Diversity partitioning of a Late Ordovician marine biotic invasion: controls on diversity in regional ecosystems. Paleobiology 33:295–309.

Pearson, P. N., and B. S. Wade. 2015. Systematic taxonomy of exceptionally well-preserved planktonic foraminifera from the Eocene/Oligocene boundary of Tanzania. Pp. 1–85 *in* Cushman Foundation for Foraminiferal Research, Vol. 45. GeoScience World, McLean, Va.

Pearson, P. N., R. K. Olsson, B. T. Huber, C. Hemleben, and W. A. Berggren. 2006. Atlas of Eocene planktonic foraminifera. Cushman Foundation for Foraminiferal Research, Lawrence, Kans.

Pearson, P. N., I. K. Mcmillan, B. S. Wade, T. D. Jones, H. K. Coxall, P. R. Bown, and C. H. Lear. 2008. Extinction and environmental change across the Eocene–Oligocene boundary in Tanzania. Geology 36:179–182.

Petrizzo, M. R., G. Leoni, R. P. Speijer, B. De Bernardi, and F. Felletti. 2008. Dissolution susceptibility of some Paleogene planktonic foraminifera from ODP Site 1209 (Shatsky Rise, Pacific Ocean). Journal of Foraminiferal Research 38:357–371.

Petro, S. M., M. A. Pivel, and J. C. Coimbra. 2018. Foraminiferal solubility rankings: a contribution to the search for consensus. Journal of Foraminiferal Research 48:301–313.

Pfuhl, H. A., and N. J. Shackleton. 2004. Two proximal, high-resolution records of foraminiferal fragmentation and their implications for changes in dissolution. Deep-Sea Research, part I (Oceanographic Research Papers) 51:809–832.

Preston, F. W. 1948. The commonness, and rarity, of species. Ecology 29:254–283.

https://doi.org/10.1017/pab.2022.24 Published online by Cambridge University Press

Purvis, A., and A. Hector. 2000. Getting the measure of biodiversity. Nature 405:212–219.

R Core Team. 2020. R: a language and environment for statistical computing. R Foundation for Statistical Computing, Vienna, Austria.

Raia, P., F. Carotenuto, A. Mondanaro, S. Castiglione, F. Passaro, F. Saggese, M. Melchionna, C. Serio, L. Alessio, D. Silvestro, and M. Fortelius. 2016. Progress to extinction: increased specialisation causes the demise of animal clades. Scientific Reports 6:1–10.

Rasmussen, C. M. Ø., B. Kröger, M. L. Nielsen, and J. Colmenar. 2019. Cascading trend of Early Paleozoic marine radiations paused by Late Ordovician extinctions. Proceedings of the National Academy of Sciences USA 116:7207–7213.

Reich, P. B., D. Tilman, F. Isbell, K. Mueller, S. E. Hobbie, D. F. B. Flynn, and N. Eisenhauer. 2012. Impacts of biodiversity loss escalate through time as redundancy fades. Science 336:589–592.

Reydon, T. A. C. 2019. Are species good units for biodiversity studies and conservation efforts? Pp. 167–193 *in* E. Casetta, J. Marques da Silva, and D. Vecchi, eds. From assessing to conserving biodiversity: conceptual and practical challenges. Springer International Publishing, Cham, Switzerland.

Rivero-Cuesta, L., T. Westerhold, C. Agnini, E. Dallanave, R. H. Wilkens, and L. Alegret. 2019. Paleoenvironmental changes at ODP Site 702 (South Atlantic): anatomy of the Middle Eocene Climatic Optimum. Paleoceanography and Paleoclimatology 34:2047–2066.

Rolland, J., and N. Salamin. 2016. Niche width impacts vertebrate diversification. Global Ecology and Biogeography 25:1252–1263.

Rutherford, S., S. D'Hondt, and W. Prell. 1999. Environmental controls on the geographic distribution of zooplankton diversity. Nature 400:749–753.

Savian, J. F., L. Jovane, F. Frontalini, R. I. F. Trindade, R. Coccioni, S. M. Bohaty, P. A. Wilson, F. Florindo, A. P. Roberts, R. Catanzariti, and F. Iacoviello. 2014. Enhanced primary productivity and magnetotactic bacterial production in response to middle Eocene warming in the Neo-Tethys Ocean. Palaeogeography, Palaeoclimatology, Palaeoecology 414:32–45.

Schiebel, R., and C. Hemleben. 2001. Classification and taxonomy of extant planktic foraminifers. Pp. 11–110 *in* R. Schiebel and C. Hemleben, eds. Planktic foraminifers in the modern ocean. Springer, Berlin.

Schiebel, R., and C. Hemleben. 2008. Protozoa, planktonic foraminifera. Pp. 606–612 *in* J. H. Steele, ed. Encyclopedia of ocean sciences, 2nd ed. Academic Press, London.

Schmidt, D. N., S. Renaud, and J. Bollmann. 2003. Response of planktic foraminiferal size to late Quaternary climate change. Paleoceanography 18:1–12.

Schmidt, D. N., H. R. Thierstein, and J. Bollmann. 2004. The evolutionary history of size variation of planktic foraminiferal assemblages in the Cenozoic. Palaeogeography, Palaeoclimatology, Palaeoecology 212:159–180.

Sexton, P. F., P. A. Wilson, and P. N. Pearson. 2006. Palaeoecology of late middle Eocene planktic foraminifera and evolutionary implications. Marine Micropaleontology 60:1–16.

Smith, A. B., and C. H. Jeffery. 1998. Selectivity of extinction among sea urchins at the end of the Cretaceous period. Nature 392:69–71.

Steineck, P. L. 1971. Middle Eocene refrigeration—new evidence from California planktonic foraminiferal assemblages. Lethaia 4:125–129.

Takagi, H., K. Kimoto, T. Fujiki, H. Saito, C. Schmidt, M. Kucera, and K. Moriya. 2019. Characterizing photosymbiosis in modern planktonic foraminifera. Biogeosciences 16:3377–3396.

Thunell, R. C. 1976. Calcium carbonate dissolution history in Late Quaternary deep-sea sediments, western Gulf of Mexico. Quaternary Research 297:281–297.

Todd, C. L., D. N. Schmidt, M. M. Robinson, and S. D. Schepper. 2020. Planktic foraminiferal test size and weight response to the Late Pliocene environment. Paleoceanography and Paleoclimatology 35:1–15.

Van Peer, T. E., D. Liebrand, C. Xuan, P. C. Lippert, C. Agnini, N. Blum, P. Blum, P. S. M. Bohaty, P. Bown, R. Greenop, and W. E. Kordesch. 2017. Data report: revised composite depth scale and splice for IODP Site U1406. Proceedings of the Integrated Ocean Drilling Program 342:1–23.

Van Valkenburgh, B. 2004. Cope's rule, hypercarnivory, and extinction in North American canids. Science 306:101–104.

Wade, B. 2004. Planktonic foraminiferal biostratigraphy and mechanisms in the extinction of *Morozovella* in the late middle Eocene. Marine Micropaleontology 51:23–38.

Wade, B., and R. K. Olsson. 2009. Investigation of pre-extinction dwarfing in Cenozoic planktonic foraminifera. Palaeogeography, Palaeoclimatology, Palaeoecology 284:39–46.

Wade, B., and P. N. Pearson. 2008. Planktonic foraminiferal turnover, diversity fluctuations and geochemical signals across the Eocene/Oligocene boundary in Tanzania. Marine Micropaleontology 68:244–255.

Wade, B., N. Al-Sabouni, C. Hemleben, and D. Kroon. 2008. Symbiont bleaching in fossil planktonic foraminifera. Evolutionary Ecology 22:253–265.

Wade, B., R. K. Olsson, P. N. Pearson, B. T. Huber, and W. A. Berggren. 2018. Atlas of Oligocene planktonic foraminifera. Cushman Foundation for Foraminiferal Research, Vol. 46. GeoScience World, McLean, Va.

Walker, B., A. Kinzig, and J. Langridge. 1999. Plant attribute diversity, resilience, and ecosystem function: the nature and significance of dominant and minor species. Ecosystems 2:95–113.

Westerhold, T., and U. Röhl. 2013. Orbital pacing of Eocene climate during the Middle Eocene Climate Optimum and the chron C19r event: missing link found in the tropical western Atlantic. Geochemistry, Geophysics, Geosystems 14:4811–4825.

Westerhold, T., U. Röhl, B. Donner, and J. C. Zachos. 2018. Global extent of Early Eocene hyperthermal events: a new Pacific benthic foraminiferal isotope record from Shatsky Rise (ODP Site 1209). Paleoceanography and Paleoclimatology 33:626–642.

Westerhold, T., N. Marwan, A. J. Drury, D. Liebrand, C. Agnini, E. Anagnostou, J. S. K. Barnet, S. M. Bohaty, D. D. Vleeschouwer, F. Florindo, T. Frederichs, D. A. Hodell, A. E. Holbourn, D. Kroon, V. Lauretano, K. Littler, L. J. Lourens, M. Lyle, H. Pälike, U. Röhl, J. Tian, R. H. Wilkens, P. A. Wilson, and J. C. Zachos. 2020. An astronomically dated record of Earth's climate and its predictability over the last 66 million years. Science 369:1383–1387.

Whittaker, R. J., K. J. Willis, and R. Field. 2001. Scale and species richness: towards a general, hierarchical theory of species diversity. Journal of Biogeography 28:453–470.

Wood, S. N. 2011. Fast stable restricted maximum likelihood and marginal likelihood estimation of semiparametric generalized linear models. Journal of the Royal Statistical Society of London B 73:3–36.

Wood, S. N. 2017. Generalized additive models: an introduction with R, 2nd ed. Chapman and Hall/CRC, Boca Raton, Fla.

Yasuhara, M., H. Doi, C. Wei, R. Danovaro, and S. E. Myhre. 2016. Biodiversity—ecosystem functioning relationships in long-term time series and palaeoecological records: deep sea as a test bed. Philosophical Transactions of the Royal Society of London B 371:20150282.

Yasuhara, M., D. P. Tittensor, H. Hillebrand, and B. Worm. 2017. Combining marine macroecology and palaeoecology in understanding biodiversity: microfossils as a model. Biological Reviews 92:199–215.

https://doi.org/10.1017/pab.2022.24 Published online by Cambridge University Press

Yasuhara, M., C.-L. Wei, M. Kucera, M. J. Costello, D. P. Tittensor, W. Kiessling, T. C. Bonebrake, C. R. Tabor, R. Feng, A. Baselga, K. Kretschmer, B. Kusumoto, and Y. Kubota. 2020. Past and future decline of tropical pelagic biodiversity. Proceedings of the National Academy of Sciences USA 117:12891–12896.

Zachos, J. C., T. M. Quinn, and K. A. Salamy. 1996. High-resolution (104 years) deep-sea foraminiferal stable isotope records of the Eocene–Oligocene climate transition. Paleoceanography 11:251–266.

Zar, J. H. 2010. Biostatistical analysis, 5th ed. Prentice Hall, Upper Saddle River, N.J.

https://doi.org/10.1017/pab.2022.24 Published online by Cambridge University Press